ChemPubSoc Europe

DOI: 10.1002/cmdc.201402291

Benzofuran–Chalcone Hybrids as Potential Multifunctional Agents against Alzheimer's Disease: Synthesis and in vivo Studies with Transgenic *Caenorhabditis elegans*

Koneni V. Sashidhara,*[a] Ram K. Modukuri,[a] Pooja Jadiya,[b] Ranga Prasad Dodda,[a] Manoj Kumar,[a] Balasubramaniam Sridhar,[c] Vikash Kumar,[d] Rizwanul Haque,[b] Mohammad Imran Siddiqi,[d] and Aamir Nazir*[b]

This paper is dedicated to Prof. Chhitar Mal Gupta (Former Director) on the occasion of his 70th birthday and to honor him for his dedicated services to Central Drug Research Institute, in his long and illustrious career.

In the search for effective multifunctional agents for the treatment of Alzheimer's disease (AD), a series of novel hybrids incorporating benzofuran and chalcone fragments were designed and synthesized. These hybrids were screened by using a transgenic *Caenorhabditis elegans* model that expresses the human β-amyloid (Aβ) peptide. Among the hybrids investigated, (*E*)-3-(7-methyl-2-(4-methylbenzoyl)benzofuran-5-yl)-1-phenylprop-2-en-1-one (**4 f**), (*E*)-3-(2-benzoyl-7-methylbenzofuran-5-yl)-1-phenylprop-2-en-1-one (**4 i**), and (*E*)-3-(2-benzoyl-7-methylbenzofuran-5-yl)-1-(thiophen-2-yl)prop-2-en-1-one (**4 m**) significantly decreased Aβ aggregation and increased acetylcholine (ACh) levels along with the overall availability of ACh at the synaptic junction. These compounds were also found to decrease acetylcholinesterase (AChE) levels, reduce oxidative stress in the worms, lower lipid content, and to provide protection against chemically induced cholinergic neurodegeneration. Overall, the multifunctional effects of these hybrids qualify them as potential drug leads for further development in AD therapy.

Introduction

Alzheimer's disease (AD) is one of the most common fatal neurodegenerative disorders for which no cure is known.[1] Irreversible memory loss, disorientation, language impairment, and cognitive decline are the most common clinical symptoms associated with AD. The pathological hallmarks of AD include extracellular β-amyloid (Aβ) plaque formation (containing mainly $A\beta_{1-42}$) and the formation of neurofibrillary tangles (containing hyperphosphorylated tau protein).[2] Moreover, oxidative stress, mitochondrial dysfunction, and impairment of protein degradation accelerate disease progression significantly.[3] Current therapeutic treatments for AD are focused on the symptomatic aspects of the pathology, as they are limited primarily to acetylcholinesterase (AChE) inhibitors, namely donepezil, rivastigmine, and galantamine.[4] These drugs modulate a single target, and therefore enable only palliative treatment rather than a cure or prevention of AD.[5] The complexity and manifold pathogenesis of AD[6] have prompted researchers to move from the traditional *one protein, one target, one drug* strategy to a new paradigm in drug research involving a multitarget-directed ligand (MTDL) design strategy.[7] Therefore, researchers are now turning to the design of hybrid structures that should be able to simultaneously interact with multiple targets.[8]

Benzofuran derivatives are pivotal biodynamic agents from both synthetic and natural sources.[9] New egonol-type benzofurans were recently isolated from natural sources, and have shown significant inhibition of AChE and AChE-induced Aβ aggregation.[10] Furthermore, a literature survey of the scaffold revealed that benzofuran-ring-containing derivatives (SKF-64346 and aminostyrylbenzofuran derivatives) exhibited inhibitory activity toward Aβ fibril formation.[11,12] Alternatively, chalcones (1,3-diaryl-2-propen-1-ones) are an important class of plant secondary metabolites and possess a wide range of biological activities.[13] It has been reported that chalcone derivatives are

[a] *Dr. K. V. Sashidhara, R. K. Modukuri,[+] R. P. Dodda, Dr. M. Kumar*
Medicinal and Process Chemistry Division
CSIR-Central Drug Research Institute (CSIR-CDRI)
Jankipuram Extension, Sitapur Road, Lucknow 226031 (India)
E-mail: kv_sashidhara@cdri.res.in

[b] *P. Jadiya,[+] R. Haque, Dr. A. Nazir*
Laboratory of Functional Genomics and Molecular Toxicology
Division of Toxicology, CSIR-Central Drug Research Institute (CSIR-CDRI)
Jankipuram Extension, Sitapur Road, Lucknow 226031 (India)
E-mail: anazir@cdri.res.in

[c] *Dr. B. Sridhar*
Laboratory of X-ray Crystallography
CSIR-Indian Institute of Chemical Technology (CSIR-IICT)
Hyderabad, 500007 (India)

[d] *V. Kumar, Dr. M. I. Siddiqi*
CSIR-Central Drug Research Institute (CSIR-CDRI)
Jankipuram Extension, Sitapur Road, Lucknow 226031 (India)

[+] *These authors contributed equally to this work.*

Supporting information for this article is available on the WWW under http://dx.doi.org/10.1002/cmdc.201402291: details of compound synthesis, characterization, HPLC analyses, X-ray crystallographic information, and docking procedures.

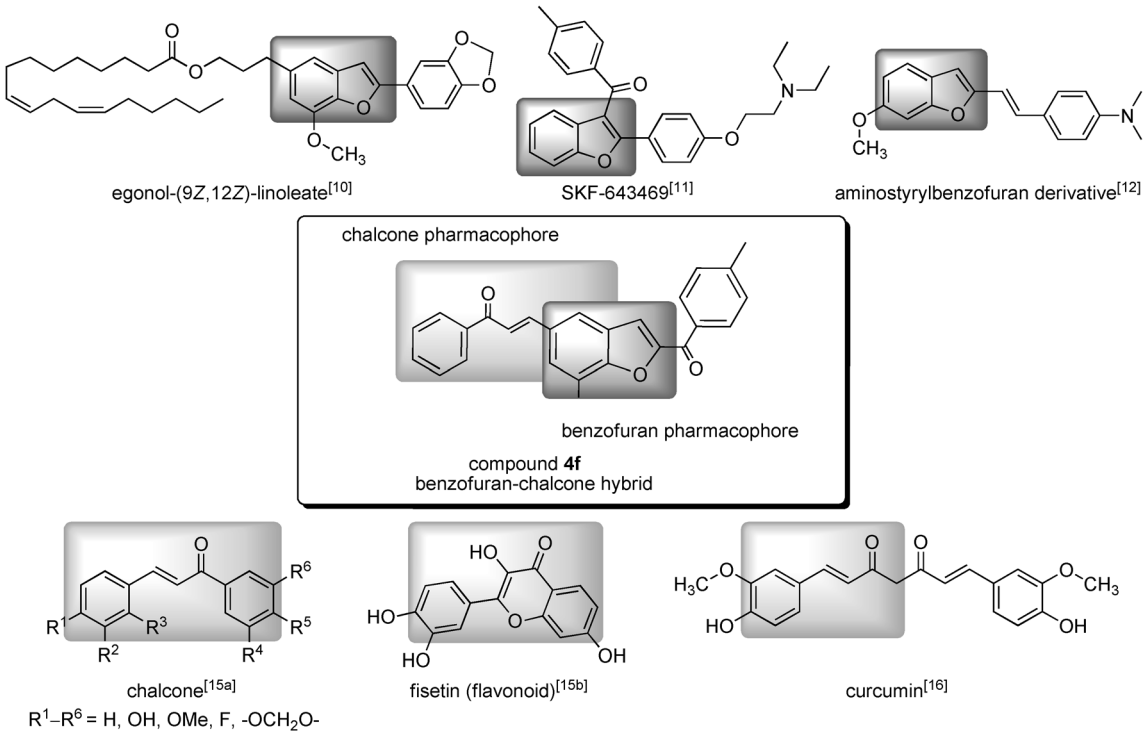

Figure 1. Design of benzofuran–chalcone hybrids for the treatment of AD.

able to directly scavenge a variety of reactive oxygen species (ROS) and possess strong antioxidant properties.[14] Recent evidence has suggested that chalcone derivatives have the capacity to inhibit Aβ fibril formation and exert neuroprotection.[15] Interestingly, curcuminoids, a class of chalcone, have been shown to exhibit potent inhibitory effects on Aβ-induced oxidative stress.[16] Therefore, introducing a chalcone pharmacophore into a hybrid molecule could impart it with neuroprotective effects and the capacity to decrease oxidative stress, which are crucial properties to halt the progression of AD.[17] Our research group has been involved for many years in the rational design and synthesis of several new multifunctional compounds by using the concept of molecular hybridization.[18,19] Herein we describe the synthesis and pharmacological evaluation of novel benzofuran-based chalcone hybrids as potential multitargeted agents for the treatment of AD. Figure 1 shows representative potent inhibitors that contain benzofurans and chalcones in their molecular makeup along with structures of our designed hybrids.

We carried out the evaluation of these hybrids in a transgenic *C. elegans* model expressing "human" Aβ.[20] This model has been used for studying Aβ toxicity in relevance to age-related disorders due to the organism's short life cycle and experimental flexibility.[21] This model exhibits toxic effects via aggregation of Aβ and has been reported to have a proteomic expression pattern, similar to that of postmortem brain tissue from human AD patients.[22] *C. elegans* is extremely relevant in AD research, as the first ever genetic understanding of the disease came from this model when the presenilin-1 (PS-1) homologue *sel-12* was identified. The gene is now known to be conserved between these nematodes and humans, as the phenotype in the *C. elegans sel-12* mutant was shown to be complemented by the expression of human PS-1.[23] *C. elegans* is also valuable to the study of neurodegenerative diseases, as it provides an uncomplicated in vivo nervous system for the study of many genes involved in its neuronal function—genes that have closely related human homolgues.

This *C. elegans* model provided a platform for us to examine the effects of our novel benzofuran–chalcone hybrids on multiple factors such as Aβ aggregation, acetylcholine (ACh) and AChE levels, the availability of ACh at the synaptic junction, oxidative stress, mitochondrial content, and lipid depositions.

Results and Discussion

Chemistry

The synthetic routes used for preparation of the target and intermediate compounds are depicted in Scheme 1. Although the synthesis of 2-substituted benzofuran-based chalcones were reported recently,[24] for this study we used a new, general, and more efficient route for the synthesis of 5-substituted benzofuran–chalcone hybrids starting from our versatile dicarbaldehyde intermediate **2**.[25]

Duff formylation on *ortho*-cresol in the presence of hexamethylenetetraamine (HMTA) and trifluoroacetic acid (TFA) at 120 °C gave the aromatic dicarbaldehyde **2**.[18] Next, Rap–Stoermer condensation[26] on compound **2** with various phenacyl bromides in the presence of potassium carbonate furnished the benzofuran carbaldehyde derivatives **3a–c** in quantitative yields. Introduction of the chalcone scaffold was carried out by reaction of various acetophenones in methanolic potassium

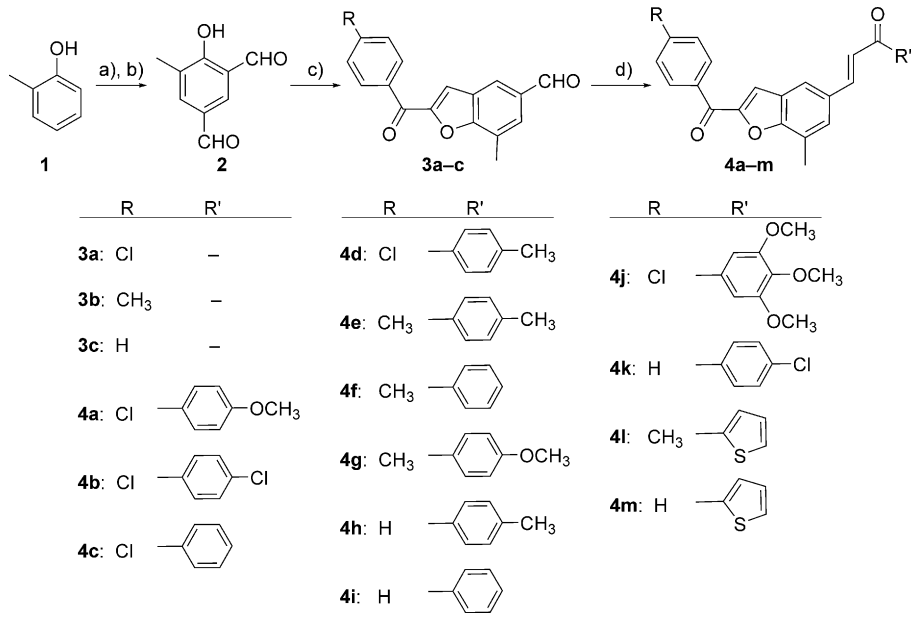

Scheme 1. Synthesis of substituted benzofuran–chalcone hybrids. *Reagents and conditions*: a) HMTA, TFA, 120 °C, 3 h; b) H_2SO_4 (aq. 10%), 100 °C, 2 h; c) various substituted phenacyl bromides, K_2CO_3/CH_3CN, 110 °C, 3 h; d) various substituted acetophenones, KOH (10% in MeOH), 3 h, RT.

hydroxide at room temperature to give the final benzofuran–chalcone hybrids **4a**–**m**. The structures of the compounds were verified by ^{1}H NMR, ^{13}C NMR, mass spectrometry, and IR spectroscopy. Additionally, the structure of a representative compound, **4d**, was distinctly confirmed by single-crystal X-ray analysis (Figure 2; see the Supporting Information for further details).

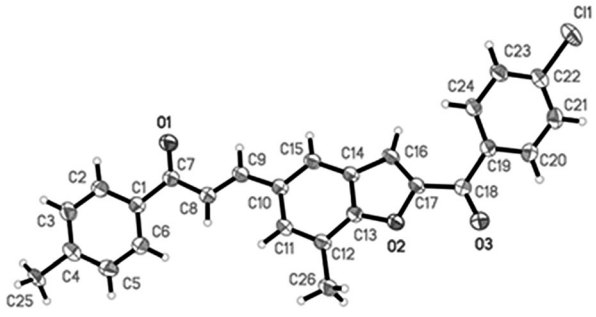

Figure 2. X-ray crystallographic structure of compound **4d**.

Biological assays

Benzofuran–chalcone hybrids decrease Aβ-induced toxicity in a transgenic C. elegans *model expressing human Aβ*

AD is characterized by aggregation of the Aβ peptide. Therefore, we performed this experiment with a transgenic *C. elegans* strain (CL4176), which exhibits temperature-inducible expression of human Aβ. The strain has been designed to express Aβ specifically in the muscles; therefore, increased Aβ in the worms leads to early paralysis, which makes an easy endpoint to screen the effect of a compound on Aβ aggregation. The effect of test compounds on the paralysis phenotype of transgenic CL4176 nematodes is presented in Figure 3. Out of the 16 compounds evaluated, seven decreased Aβ aggregation, leading to a delay in paralysis by 2- ($p<0.01$), 1.4- ($p<0.05$), 2.3- ($p<0.01$), 1.7- ($p<0.01$), 1.4- ($p<0.05$), 1.8- ($p<0.01$), and 2.1-fold ($p<0.01$) in worms fed with compounds **3a**, **4c**, **4d**, **4f**, **4i**, **4l** and **4m**, respectively. In this study, all compounds were screened in the presence of control as well as vehicle control, and compounds that did not affect Aβ-induced paralysis were not selected for further studies.

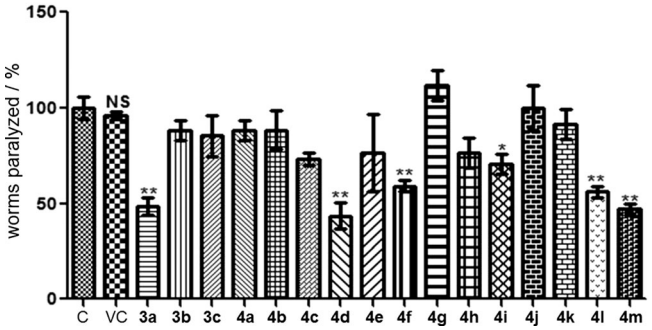

Figure 3. Aβ-induced paralysis assay in the CL4176 strain of *C. elegans* treated with the indicated test compounds. Control (C) = OP50 only; vehicle control (VC) = ethanol. Data are normalized with respect to control, and values are the mean ± SEM of $n=3$ experiments performed in triplicate; $^*p<0.05$, $^{**}p<0.01$.

It is well known that AChE is the key enzyme responsible for the metabolic and catalytic hydrolysis of ACh and for promoting the aggregation and deposition of Aβ peptide.[27] This prompted us to speculate that the reduced Aβ aggregation observed is due to the effect of our hybrids on the aggregation of Aβ and its associated toxicity. This decrease in Aβ aggregation could also be associated with the binding affinity of the benzofuran scaffold to Aβ, as it has been reported to inhibit the polymerization process that leads to amyloid neurotoxicity.

Benzofuran–chalcone hybrids enhance ACh availability/excitatory neurotransmission in wild-type C. elegans

AD is tightly associated with impaired synthesis of the excitatory neurotransmitter, ACh. Therefore, we endeavored to study

the role of our test compounds in enhancing ACh levels in the *C. elegans* model. A pharmacological assay was performed to determine the effect of hybrids on the release of ACh in the synaptic cleft. AChE, present at the synaptic cleft, is known to catalyze the hydrolysis of ACh into choline and acetate, thus eliminating the neurotransmitter from the synapse. In the presence of an AChE inhibitor, aldicarb, the hydrolysis of ACh is prevented, thus leading to its continued accumulation at the synapse. This, in turn, causes flexing of muscles thereby paralyzing the worms. This assay is known as the aldicarb assay, which gives a rapid assessment of the effect of pharmacological and toxicological agents on the ACh content in nematodes. As shown in Figure 4, exposure of worms with compounds **4f**, **4i**, and **4m** exhibited a significant ($p<0.05$) increase in the availability of ACh at the synapse, which in turn led to early aldicarb-induced paralysis. Compound **4f** showed a 1.6-fold increase in ACh levels relative to the standard AChE inhibitor donepezil. Compounds **4i** and **4m** exhibited an increase in the availability of ACh nearly equal to that of donepezil. Similarly, donepezil-, **4f**-, **4i**-, and **4m**-treated worms displayed 1.8-, 2.8-, 1.6-, and 1.9-fold increased ACh availability respectively, in comparison with control worms. This experiment showed that the hybrid molecules **4f**, **4i**, and **4m** are potent, vis-à-vis increasing ACh availability, than the parent benzofuran compound **3a**.

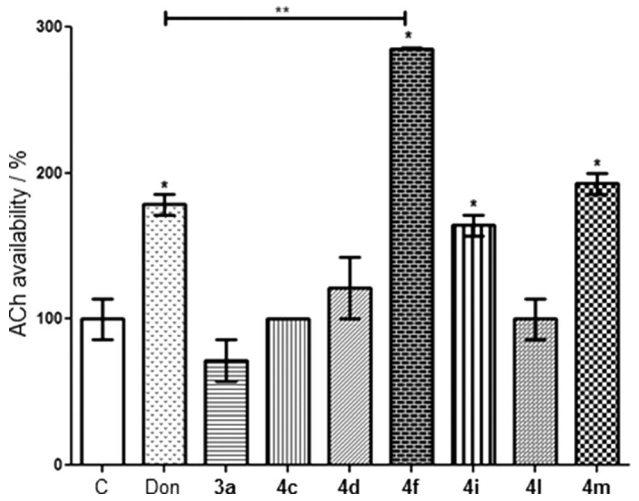

Figure 4. Effect of the test compounds on acetylcholine availability as determined by the aldicarb assay in the N2 strain of *C. elegans*. C = vehicle control (ethanol); Don = donepezil. Data are normalized with respect to control, and values are the mean ± SEM of $n=3$ experiments performed in triplicate; $^{*}p<0.05$, $^{**}p<0.01$.

In the central nervous system (CNS), ACh, released from cholinergic neurons, plays a significant role in maintaining cognition, memory, and learning. Impaired neurotransmission and decreased levels of ACh contribute to the pathology of AD.[28] Therefore, compounds that enhance the release of ACh could be further explored as potential treatments for the cognitive symptoms of AD. In our study, compounds **4f**, **4i**, and **4m** increased the levels of ACh, demonstrating that the hybrids increase the availability of ACh, thus aiding in improved excitatory neurotransmission. Because **4f**, **4i**, and **4m** showed their potential both in blocking Aβ aggregation and in enhancing ACh availability, we carried out further biological studies with these three compounds to explore their multifactorial potential against AD.

Benzofuran–chalcone hybrids increase ACh and inhibit AChE activity in C. elegans

We further estimated the levels and activity of ACh and AChE in control and test-compound-treated worms along with negative and positive controls (provided with the assay kit; see Experimental Section below). As depicted in Figure 5A, treatment of worms with compounds **4f**, **4i**, and **4m** gave significantly higher ACh levels than untreated worms. Exposure of worms with compounds **4f**, **4i**, and **4m** showed respective 1.3- ($p<0.001$), 1.5- ($p<0.001$), and 1.1-fold ($p<0.05$) increased ACh levels. In further quantification of AChE inhibition, **4f**- and **4i**-treated worms showed significant inhibition of AChE activity. Inhibition of AChE activity was significantly ($p<0.001$) decreased in **4f**- (1.7-fold) and **4i**- (2.3-fold) treated worms, relative to control. Worms raised on compound **4m** exhibited maximum inhibition of AChE, showing 10.7-fold decrease in comparison with untreated worms ($p<0.001$; Figure 5B).

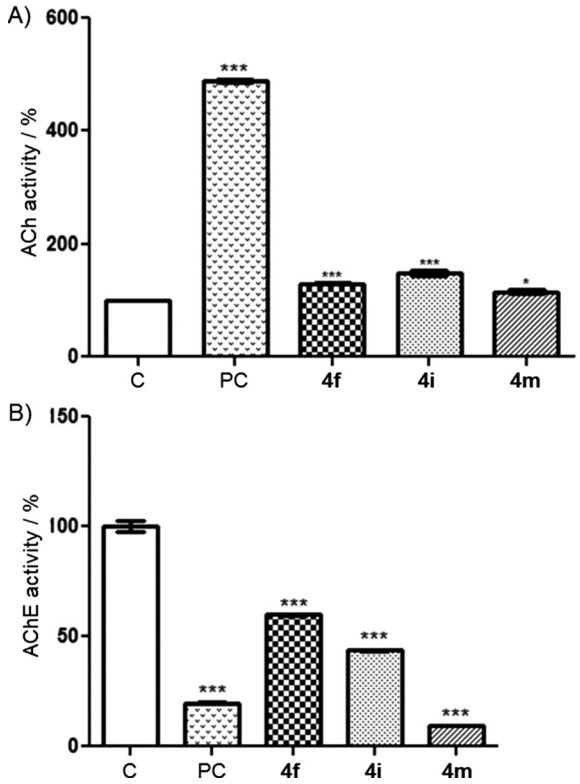

Figure 5. Effect of test compounds on A) acetylcholine and B) acetylcholinesterase activities, as measured by the Amplex® Red assay in wild-type *C. elegans*. Control (C) = OP50 only; positive control (PC) = for ACh activity 10 μM H_2O_2 and for AChE activity 0.2 U mL^{-1} AChE solution. Data are normalized with respect to control, and values are the mean ± SEM of $n=2$ experiments performed in triplicate; $^{*}p<0.05$, $^{***}p<0.001$.

These studies gave evidence that the benzofuran–chalcone hybrids inhibit AChE and also increase the levels of ACh via other mechanisms, probably by increasing biosynthesis of the neurotransmitter or by blocking AChE activity.

Benzofuran–chalcone hybrids afford neuroprotection in a C. elegans *model of cholinergic neurodegeneration*

In this study, we employed transgenic LX929 (*unc-17*: green fluorescent protein (GFP)) strain of *C. elegans* that expresses GFP specifically in cholinergic neurons. In *C. elegans* more than a third of neuronal cells are cholinergic neurons, and thus ACh is the main excitatory neurotransmitter to release at neuromuscular junctions. The organophosphate pesticide chlorpyrifos (CP) is known to induce cholinergic damage; therefore, we used this model to study the effects of our hybrids for the prevention of CP-induced cholinergic neuronal damage. As shown in Figure 6A, control worms displayed complete cholinergic neuroanatomy, whereas treatment with CP resulted in a loss of the GFP expression pattern due to CP-induced cholinergic neurodegeneration (Figure 6B). This neurodegeneration was significantly ($p < 0.001$) prevented if worms were fed on test compound CP–**4f**; a 1.6-fold increase in cholinergic neuroprotection was observed relative to that of CP-treated worms (Figure 6C). Similarly, if raised on CP–**4i** and CP–**4m**, worms exhibited a 1.3- ($p < 0.05$) and 1.5-fold ($p < 0.01$) increase in cholinergic neuroprotection relative to that of worms from the CP-treated group (Figure 6D,E), this evaluation led us to conclude the potential of these compounds in improving cholinergic neurophysiology.[29–34] The neuroprotection observed in our studies could also be due to decreased aggregation of Aβ, as it is well known that increased Aβ deposition leads to neuronal death via a number of possible mechanisms, including oxidative stress.[35]

Benzofuran–chalcone hybrids inhibit Aβ deposits in transgenic C. elegans

Aβ aggregate formation plays a central role in the pathogenesis of AD. To determine whether the benzofuran–chalcone hybrids have any effect on Aβ oligomerization in the transgenic *C. elegans* strain CL2006, which expresses human Aβ under control of the *unc-54* promoter (encodes a muscle myosin class II heavy chain (MHC B)), worms were fed with the test compound and subjected to Aβ staining by thioflavin S. Thioflavin S is used for staining of amyloid plaques; it binds to Aβ fibrils (but not monomers) and gives a distinct spectral shift upon binding.[36] The Aβ deposits (highlighted by arrows) without test compound can clearly be seen in Figure 7A. In contrast, worms fed with benzofuran–chalcone hybrids **4f**, **4i**, and **4m** showed a significant decrease in Aβ deposits (Figure 7B–D).

The inhibitory effect of these compounds was scored by counting the number of plaque deposits per worm. We found that the mean number of Aβ deposits was significantly reduced in Aβ-expressing transgenic *C. elegans* strain fed with **4f** ($p < 0.01$), **4i** ($p < 0.05$), and **4m** ($p < 0.01$) relative to unfed controls. These results suggested that the benzofuran–chalcone hybrids inhibit Aβ oligomerization efficiently.

Dose–dependent antioxidant properties

To further explore the role of compounds **4f**, **4i**, and **4m**, which effected a significant delay in Aβ-induced paralysis as

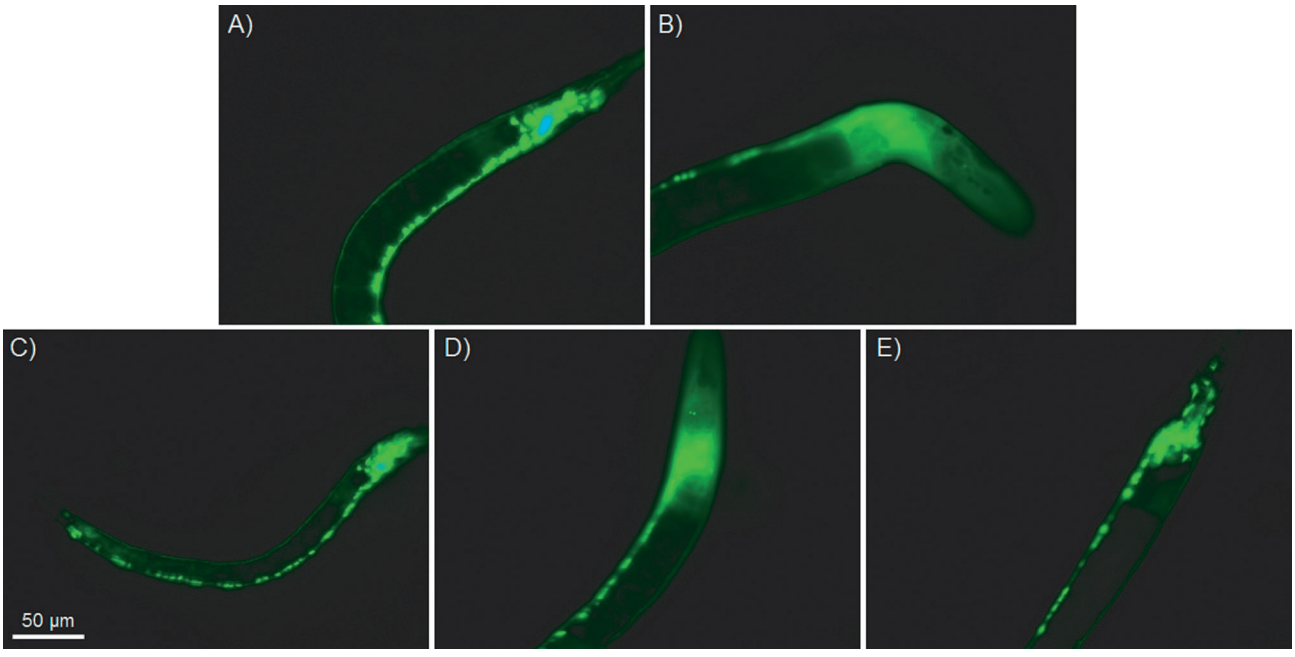

Figure 6. GFP expression pattern in cholinergic neurons of the transgenic LX929 strain of *C. elegans*. A) Control, B) chlorpyrifos (CP)-treated worms, and CP-treated worms raised on C) compound **4f**, D) compound **4i**, and E) compound **4m**.

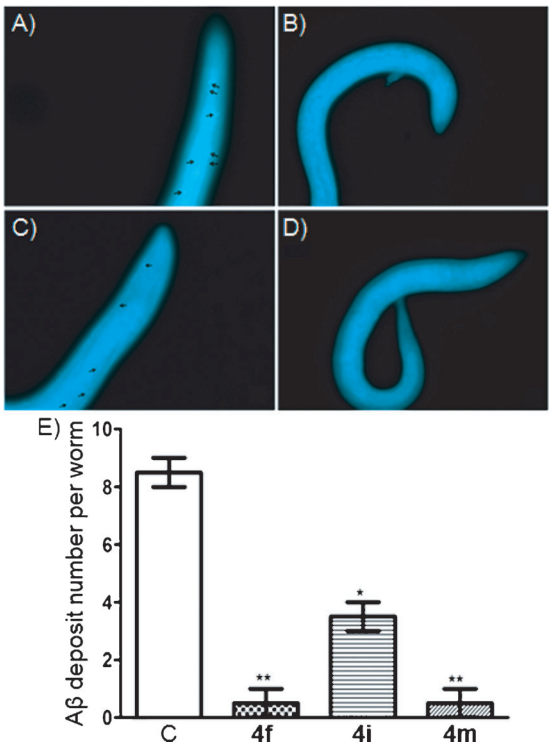

Figure 7. Thioflavin S staining to show Aβ deposits on body wall muscle (indicated by arrows). Images of Aβ deposits in A) the transgenic *C. elegans* strain CL2006 alone, and after treatment with test compounds B) **4f**, C) **4i**, and D) **4m**. E) Quantitative analysis of Aβ deposits. Control (C) = OP50 only. Data are the mean ± SEM of $n = 3$ experiments performed in triplicate; $^{*}p < 0.05$, $^{**}p < 0.01$.

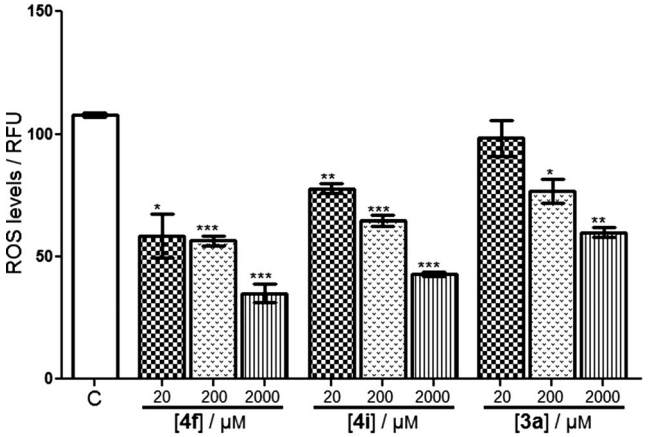

Figure 8. Effect of compounds **4f**, **4i**, and **3a** on the relative formation of reactive oxygen species as measured by H_2DCFDA assay in a transgenic CL2006 strain of *C. elegans*. C = untreated control, RFU = relative fluorescence units. Data are normalized with respect to control, and values are the mean ± SEM of $n = 3$ experiments performed in triplicate; $^{*}p < 0.05$, $^{**}p < 0.01$, $^{***}p < 0.001$.

well as an increase in the content and availability of ACh, we studied antioxidant properties using the CL2006 strain of *C. elegans*. In the case of compound **4m**, antioxidant effects were not observed in the CL2006 strain, whereas compounds **4f** and **4i** led to a significant decrease in ROS levels relative to those of untreated worms. We next studied the effect of test compound dose (**4f**, **4i**, and **3a**) on antioxidant properties using three different concentrations (20, 200, and 2000 μM) and the human-Aβ-expressing transgenic strain CL2006. Worms treated with compound **4f** showed significant 1.8- ($p < 0.05$), 1.9- ($p < 0.001$), and 3.1-fold ($p < 0.001$) decreases in ROS levels at 20, 200, and 2000 μM, respectively (Figure 8). In determining the antioxidant effects of compound **4i**, ROS levels were found to decrease 1.4- ($p < 0.05$), 1.7- ($p < 0.01$), and 2.6-fold ($p < 0.001$) in worms treated respectively at 20, 200, and 2000 μM. On the other hand, worms treated with the parent benzofuran compound **3a** at 20 μM did not show changes in ROS content, whereas at 200 and 2000 μM, worms displayed respective 1.4- ($p < 0.05$) and 1.8-fold ($p < 0.01$) decreases in ROS levels. Our results demonstrate that the hybrid molecules **4f** and **4i** exert a dose-dependent antioxidant effect across the concentration range tested.

It has been recognized for a long time that the presence of ROS increases Aβ production.[37] Therefore, use of an antioxidant can alleviate this ROS-mediated toxicity and lead to a reduction in Aβ aggregation. In our studies, compounds **4f** and **4i** decreased oxidative stress in worms; the effect was moderate in wild-type worms, whereas there was a pronounced decrease in oxidative stress in the Aβ-expressing *C. elegans* strain. This is an interesting observation, as this further corroborates the notion that benzofuran moieties possess Aβ binding properties, thus reducing the toxic effects of these aggregates. The antioxidant properties of chalcone[13] and benzofuran moieties[38] have been reported previously; some benzofuran derivatives have also been reported to exhibit protection against sulfhydryl group oxidation and lipid peroxidation.[39]

The rather specific and pronounced effect of the test compounds in our study provided evidence that the hybrid nature of these benzofuran–chalcone molecules leads to the specific decrease in oxidative stress, probably through the binding of benzofuran molecules with Aβ. Intriguingly, compound **4m** did not exhibit antioxidant properties; this implies that the observed effects of this compound are independent of effects on ROS levels and are mediated by a different pathway.

Lowering of lipid deposition in an Aβ-expressing C. elegans *strain*

High levels of lipids and altered lipid metabolism are associated with many neurodegenerative diseases, including AD.[40] We therefore studied the lipid-modulating properties of the test compounds. Using a lipid-specific fluorescent dye, Nile red, to track lipid deposits within the worms, we carried out fluorescence imaging studies using the CL2006 strain. As depicted in Figure 9, worms of the control group exhibited an optimum Nile red staining pattern (Figure 9A), whereas worms treated with compounds **4f** (Figure 9B), **4i** (Figure 9C), and **4m** (Figure 9D) showed reduced staining, thus reflecting the effect of these compounds on lipid deposition. The fluorescence intensity, as quantified by Image J analysis, for the worms of the control group was found to be 14.16 ± 1.174 arbitrary units, whereas worms treated with **4f**, **4i**, and **4m** showed fluores-

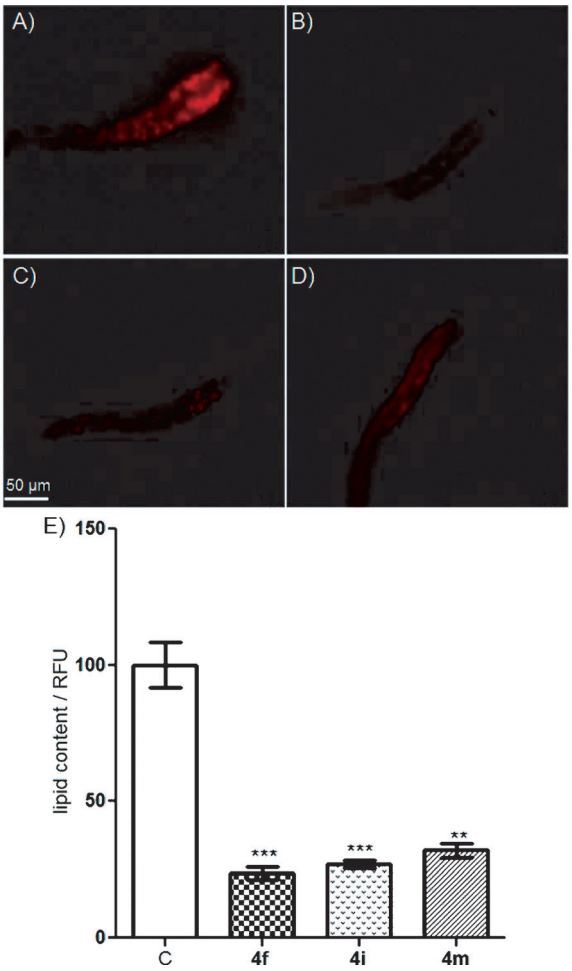

Figure 9. Nile red staining in the CL2006 strain of *C. elegans* grown on A) control diet, and treatment with test compounds B) **4 f**, C) **4 i**, and D) **4 m**. E) Relative fluorescence intensity of nematode lipid content as quantified by Image J software. C = control, RFU = relative fluorescence units. Data are normalized with respect to control, and values are the mean ± SEM of $n = 3$ experiments performed in triplicate; $^{**}p < 0.01$, $^{***}p < 0.001$.

cence intensities of 3.35 ± 0.31, 3.83 ± 0.19, and 4.53 ± 0.36 arbitrary units, thus exhibiting 4.3- ($p < 0.001$), 3.7- ($p < 0.001$), and 3.1-fold ($p < 0.01$) decreases in fluorescence intensity, respectively, relative to untreated worms (Figure 9 E). Compound **4 f** induced a rather pronounced lipid-lowering effect relative to the other two compounds, which is in agreement with the enhanced beneficial effects of this compound vis-à-vis other reported parameters of this study as well. There is sufficient published evidence linking high levels of lipids and cholesterol to amyloid fibrillogenesis and its related toxicity;[41] thus the decrease in lipid content caused by the test compounds relates well to the reduced amyloid aggregation and associated effects. Therefore, it could be assumed that the benzofuran–chalcone hybrids do affect multiple factors associated with AD.

Reduced mitochondrial content of CL2006 worms is moderately restored by compound 4 f

There is much evidence to suggest that mitochondrial dysfunction plays a causative role in the pathogenesis of AD. Furthermore, the accumulation of Aβ in the mitochondrial compartment is known to result in impairment of mitochondrial function.[3,42] Therefore, therapies targeted at protecting mitochondria may improve the clinical outcome of AD pathogenesis. In this context, we studied the effect of test compounds on mitochondrial content using Mitotracker staining. Figure 10 shows that CL2006 worms exhibited a lower mitochondrial content than wild-type worms; this was moderately restored by compound **4 f**, whereas compounds **4 i** and **4 m** did not induce any significant change in mitochondrial content. We further quantified the fluorescence intensity of mitochondrial content using Image J software. In the case of worms treated with **4 f**, a 1.2-fold increase ($p < 0.05$) in the fluorescence intensity of mito-

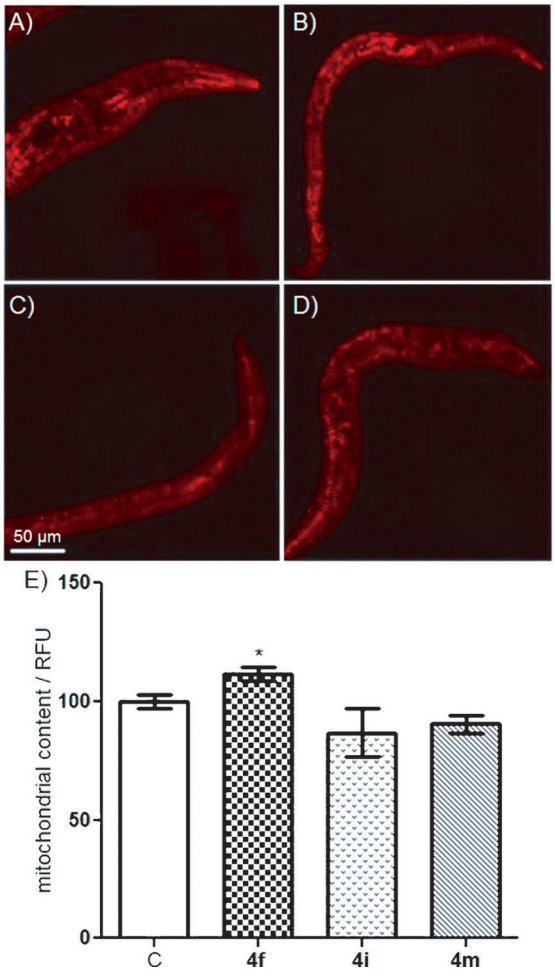

Figure 10. Mitotracker staining in the CL2006 strain of *C. elegans* fed with A) OP50, and treated with test compounds B) **4 f**, C) **4 i**, and D) **4 m**. E) Relative fluorescence intensity of nematode mitochondrial content as quantified by Image J software. C = control, RFU = relative fluorescence units. Data are normalized with respect to control, and values are the mean ± SEM of $n = 3$ experiments performed in triplicate; $^{*}p < 0.01$.

chondrial content was observed relative to the untreated transgenic CL2006 strain (Figure 10E).

Benzofuran–chalcone hybrids do not induce tissue damage in C. elegans *at tested concentrations*

Next, to examine the gross toxic effect of the test compounds, we carried out a Trypan-blue-based dye exclusion test in worms treated with compounds **4f**, **4i**, and **4m**. Trypan blue is a critical dye that is taken up by damaged cells and is excluded by cells with healthy morphology; hence the test provides a reliable assessment of cell/tissue damaging potential. We used *N*,*N*′-dimethyl-4,4′-bipyridinium dichloride (Paraquat, PQ) as a positive control for inducing cellular damage. As shown in Figure 11A, control worms exhibited a very mild staining pattern (largely background), whereas worms treated with PQ not only stained intensely (Figure 11B), but also exhibited a strong developmental effect, as the worms were developmentally impaired and smaller. Worms treated with compounds **4f** (Figure 11C), **4i** (Figure 11D), and **4m** (Figure 11E) exhibited a staining pattern similar to that of the control worms, hence depicting no cell damage.

Molecular modeling studies

The structure of *Torpedo californica* AChE (*Tc*AChE)[43] with E2020 (donepezil) has been used for many docking studies of AChE inhibitors,[44] implying that it can serve as a good model for the evaluation of newly identified compounds. In the present study, we used the *Tc*AChE–E2020 complex for analysis of the binding mode of hybrids **4f**, **4i**, and **4m** in the active site of *Tc*AChE. Re-docking with E2020 resulted in a conformation close to the co-crystal structure, with an RMSD of 0.66 Å. This validates our docking approach adopted in this study. Residues Trp84, Trp279, Trp290, and Phe330 play important roles in the binding of E2020.[43] Trp84 and Trp279 are especially significant, as both undergo a π–π stacking interaction with E2020. It has been reported that E2020 is an active site gorge spanning AChE inhibitor, interfering with both the catalytic active site (CAS) and peripheral active site (PAS) simultaneously.[45] Interestingly, docking of hybrids **4f**, **4i**, and **4m** into the active site gave almost identical positioning with respect to E2020 (Figure 12B–D), indicating that these compounds use a similar network of interactions that stabilize E2020. Figure 12 shows an ensemble of a few top-docked conformations for each compound out of 20 poses that were generated to determine any conformational preference in the active site pocket. All docked conformations were found to be similar, indicating the preferred binding mode of these compounds. At the bottom site of the binding pocket, the indole ring of Trp84 appeared to undergo π–π stacking with one of the aromatic rings of hybrids **4f**, **4i**, and **4m**. We have not observed any π–π stacking interactions with Trp279 near the entrance of active site; however the lack of this interaction was found to be compensated by hydrogen bonding of the carbonyl group of compounds with the main-chain NH group of Phe288. Residues Tyr121 and Trp279 belong to the PAS, and in the docking study we observed that the benzofuran moieties of **4f**, **4i**, and **4m** are present in close proximity to these residues. The role of PAS residues in the formation of amyloid fibrils has been reported.[46] Parent compounds **3a**, **3b**, and **3c** showed a lack of π–π stacking interactions with Trp84 in the active site of *Tc*AChE (Supporting Information Figure S1). We hypothesize that the addition of a chalcone moiety increases the stacking interactions, allowing a better positioning into the active site of *Tc*AChE. From these interaction studies, we propose that both benzofuran and chalcone moieties are essential for ACh activity and AChE inhibitory activity. These compounds also reduce

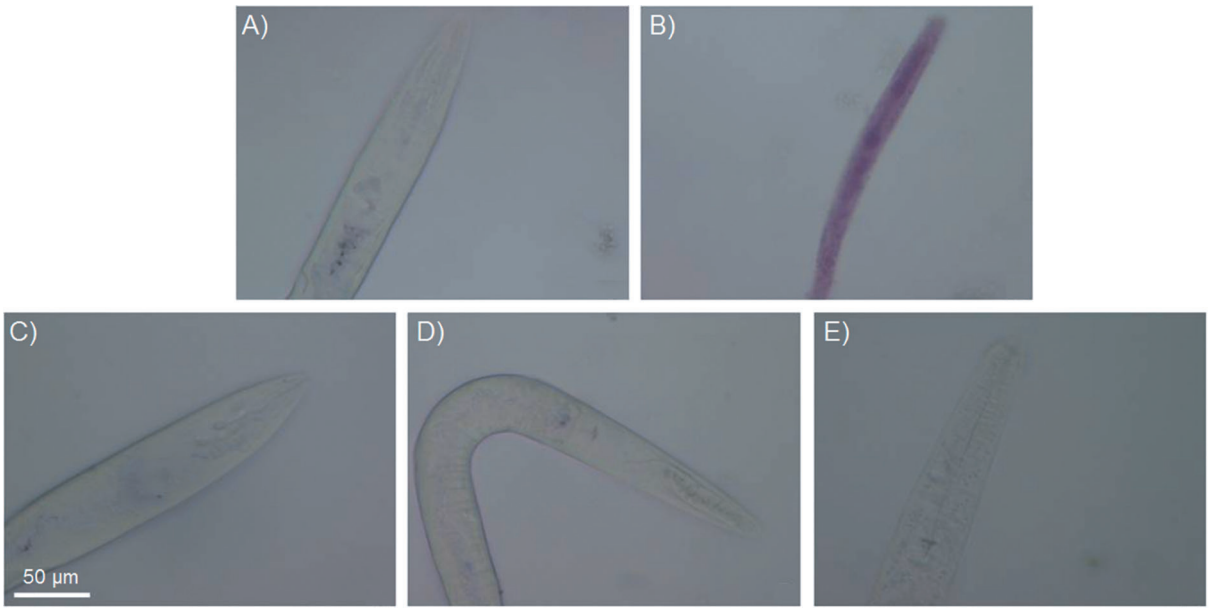

Figure 11. Cytotoxicity assay by Trypan blue staining in the N2 strain of *C. elegans*. A) Control worms, and B) PQ-treated worms raised on C) compound, **4f** D) compound **4i**, and E) compound **4m**.

Aβ aggregation which may be due to either steric blockage of ligand entry into the active site, or inducing a conformational change in the catalytic triad.

SAR of benzofuran–chalcone hybrids against Aβ aggregation

The preceding molecular modeling studies that were performed to gain insight into the binding mode revealed that both benzofuran and chalcone moieties are essential to show similar π—π stacking interactions to fit into the active site of *Tc*AChE, which stabilizes E2020. In terms of the structure–activity relationship (SAR) of the hybrids, decreased Aβ peptide aggregation was found to depend on both the substituent patterns on the phenyl ring of chalcones (R^1) and benzofuran (R). In general, on the chalcone phenyl ring (R^1), electron-donating groups (such as methoxy or methyl) seem to enhance activity. Replacement of the phenyl ring with smaller heterocyclic rings (thiophene, as in **4l** and **4m**) did not influence activity, suggesting that they share or have overlapping binding sites. On the other hand, the substitution on the phenyl ring of benzofuran (R) with a halogen (Cl; in **3a** and **4d**) increases the inhibitory potency over that of unsubstituted benzofuran hybrids (**4h** and **4k**). A summary of the SAR is depicted in Figure 13.

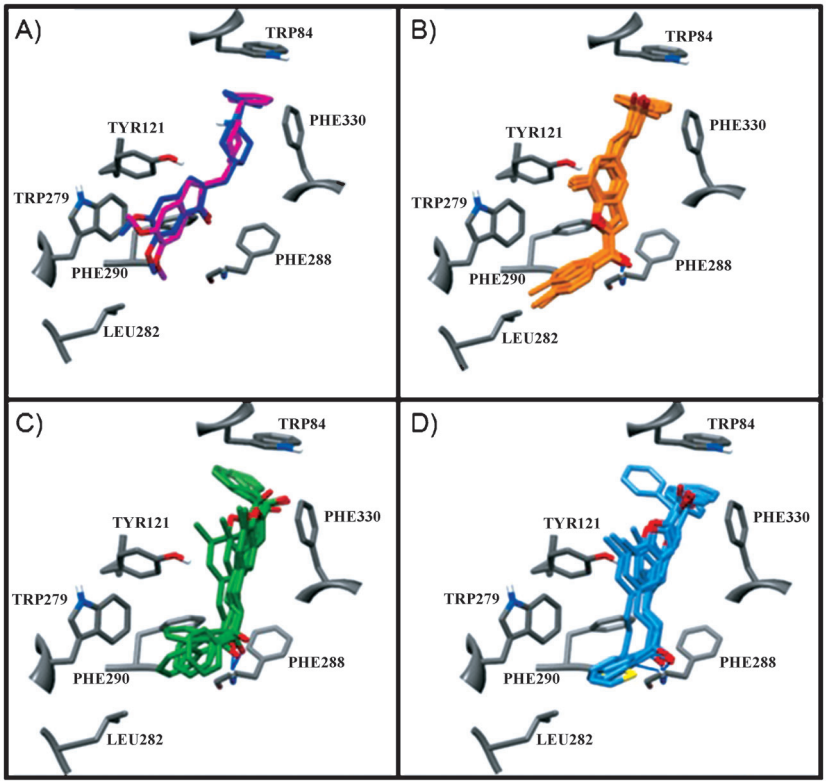

Figure 12. A) Superimposed co-crystallized (magenta) and docked conformation (blue) of E2020 in the active site of *Tc*AChE (grey). An ensemble of docked conformations, each for compounds B) **4f**, C) **4i**, and D) **4m** are shown. Only polar hydrogen atoms of *Tc*AChE are shown; other hydrogen atoms are omitted for clarity. Hydrogen bonds are indicated by blue solid lines.

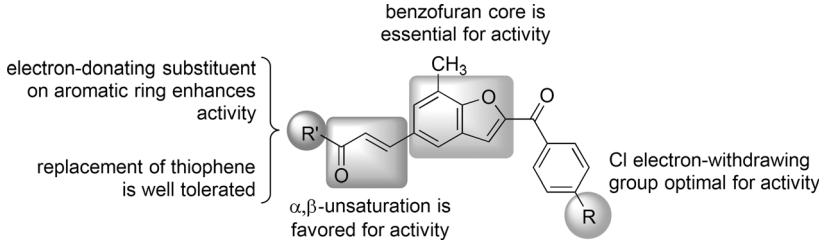

Figure 13. SAR of the synthesized hybrids against Aβ aggregation.

Conclusions

In summary, novel benzofuran–chalcone hybrids were synthesized and characterized as multifunctional agents against AD. Among the synthesized compounds, **4f**, **4i**, and **4m** significantly decreased disease effects in a transgenic *C. elegans* model of AD. The compounds exerted their beneficial effects by reducing Aβ aggregation, decreasing oxidative stress (**4f** and **4i**), increasing ACh levels, and decreasing lipid deposition, thereby preventing cholinergic neuronal degeneration. These properties highlight the therapeutic potential of these novel prototypes to be developed as new multifunctional drugs in the treatment of Alzheimer's disease.

Experimental Section

Chemistry

General: All reagents were obtained commercially and were used without further purification. Chromatography was carried out on silica gel (60–120 and 100–200 mesh). All reactions were monitored by thin-layer chromatography (TLC); silica gel plates with fluorescence F_{254} were used. Melting points were taken in open capillaries on a Complab melting point apparatus and are uncorrected. IR spectra were recorded on a PerkinElmer FT-IR RXI spectrophotometer. ^{1}H NMR and ^{13}C NMR spectra were recorded using a Bruker Supercon Magnet DRX-300 spectrometer (operating at 300 MHz for ^{1}H NMR and 75 MHz for ^{13}C NMR), with $CDCl_3$ as solvent and tetramethylsilane (TMS) as internal standard. Chemical shifts (δ) are reported in parts per million. ESIMS data were recorded on a Thermo Lcq Advantage Max-IT. HRMS data were collected on a 6520 Agi-

lent Q ToF LC–MS/MS instrument (Accurate mass). HPLC analyses for purity (>95% area) of synthesized compounds were performed on a Shimadzu instrument equipped with a Shimadzu ODS (C_{18}) reversed-phase column (4.6 mm×250 mm, 2 μm). The mobile phase was a mixture of *i*PrOH and CH_3CN. The purity of the compounds was determined by integrating peak areas of the liquid chromatogram, monitored at λ 280 and 325 nm. Parameters were as follows: flow rate: 0.4 mL min^{-1}; gradient system, from 60% *i*PrOH and 40% CH_3CN to 90% *i*PrOH and 10% CH_3CN. The solvent ratio was maintained for 30 min. All final compounds were found to have >95% purity.

2-(4-Chlorobenzoyl)-7-methylbenzofuran-5-carbaldehyde (3a): To a mixture of 4-hydroxy-5-methylisophthalaldehyde (**2**) (1.0 g, 6.09 mmol), 4-chlorophenacylbromide (1.6 g, 7.31 mmol) and K_2CO_3 (0.8 g, 6.08 mmol), CH_3CN (20 mL) was added. The reaction mixture was held at reflux for 3 h. After completion of the reaction, K_2CO_3 was removed in a sintered funnel, and the filtrate was concentrated under vacuum and purified by column chromatography with EtOAc/hexane (1:9) to give pure **3a** as a pale-yellow solid. Yield: 85%, 1.54 g; mp: 168–169 °C; $\tilde{\nu}_{max}$ (KBr) = 3020, 1691, 1646, 1600, 1217, 777 cm^{-1}; ^{1}H NMR ($CDCl_3$, 300 MHz): δ = 10.04 (s, 1H), 8.09 (s, 1H), 8.03 (d, J = 8.6 Hz, 2H), 7.86 (s, 1H), 7.63 (s, 1H), 7.53 (d, J = 8.6 Hz, 2H), 2.65 ppm (s, 3H); ^{13}C NMR ($CDCl_3$, 75 MHz): δ = 191.4, 182.5, 158.2, 153.3, 139.8, 135.0, 133.4, 131.0, 129.1, 128.9, 126.8, 124.9, 124.1, 116.7, 15.2 ppm; ESIMS (*m/z*): 299 $[M+H]^+$; HRMS *m/z* calcd for $C_{17}H_{11}ClO_3$ $[M+H]^+$ 299.0475, found 299.0461.

7-Methyl-2-(4-methylbenzoyl)benzofuran-5-carbaldehyde (3b): This compound was synthesized by the method described for compound **3a**, employing compound **2** (1.0 g, 6.09 mmol), 4-methylphenacylbromide (1.5 g, 7.31 mmol), and K_2CO_3 (0.8 g, 6.0 mmol) to afford compound **3b**. Pale-yellow solid; yield: 80%, 1.35 g; mp: 165–166 °C; $\tilde{\nu}_{max}$ (KBr) = 3043, 1684, 1659, 1629, 1204, 755 cm^{-1}; ^{1}H NMR ($CDCl_3$, 300 MHz): δ = 10.05 (s, 1H), 8.08 (s, 1H), 7.99 (d, 2H, J = 8.1 Hz), 7.84 (s, 1H), 7.60 (s, 1H), 7.35 (d, J = 8.1 Hz, 2H), 2.66 (s, 3H), 2.47 ppm (s, 3H); ^{13}C NMR ($CDCl_3$, 75 MHz): δ = 191.4, 183.5, 158.2, 153.8, 144.3, 134.2, 133.3, 128.7, 126.9, 124.8, 124.1, 116.3, 21.8, 15.2 ppm; ESIMS (*m/z*): 279 $[M+H]^+$; HRMS *m/z* calcd for $C_{18}H_{14}O_3$ $[M+H]^+$ 279.1021, found 279.1017.

2-Benzoyl-7-methylbenzofuran-5-carbaldehyde (3c): This compound was synthesized by the method described for compound **3a**, employing compound **2** (1.0 g, 6.09 mmol), phenacyl bromide (1.4 g, 7.28 mmol) and K_2CO_3 (0.8 g, 6.0 mmol) to afford compound **3c**. White solid; yield: 89%, 1.43 g; mp: 163–164 °C; $\tilde{\nu}_{max}$ (KBr) = 3028, 1677, 1665, 1615, 1229, 768 cm^{-1}; ^{1}H NMR ($CDCl_3$, 300 MHz): δ = 10.06 (s, 1H), 8.10–8.05 (m, 3H), 7.86 (s, 1H), 7.69–7.54 (m, 4H), 2.68 ppm (s, 3H); ^{13}C NMR ($CDCl_3$, 75 MHz): δ = 191.4, 183.9, 158.3, 153.6, 136.9, 133.4, 133.3, 129.5, 128.9, 128.7, 126.9, 124.9, 124.2, 116.8, 15.2 ppm; ESIMS (*m/z*): 265 $[M+H]^+$; HRMS *m/z* calcd for $C_{17}H_{12}O_3$ $[M+H]^+$ 265.0865, found 265.0855.

(*E*)-13-(2-(4-Chlorobenzoyl)-7-methylbenzofuran-5-yl)-1-(4-methoxyphenyl)prop-2-en-1-one (4a): To a mixture of 2-(4-chlorobenzoyl)-7-methylbenzofuran-5-carbaldehyde (**3a**) (1.0 g, 3.35 mmol) and 4-methoxyacetophenone (0.6 g, 4.0 mmol), 10% methanolic KOH (15 mL) was added. The reaction mixture was stirred at room temperature for 3 h. After completion of the reaction (TLC monitoring) the reaction mixture was poured into 10% dilute HCl solution (15 mL) and extracted with $CHCl_3$, dried over Na_2SO_4; removal of the solvent afforded crude compound. The crude product was purified by column chromatography with EtOAc/hexane (2:8) to provide pure **4a**. Pale-yellow solid; yield: 69%, 0.99 g; mp: 178–179 °C; $\tilde{\nu}_{max}$ (KBr) = 3021, 2927, 1705, 1645, 1595, 1550, 1285, 768 cm^{-1}; ^{1}H NMR ($CDCl_3$, 300 MHz): δ = 8.06–8.01 (m, 4H), 7.85 (d, J = 15.6 Hz, 1H), 7.77 (s, 1H), 7.61 (s, 1H), 7.57–7.50 (m, 4H), 6.98 (d, J = 8.85 Hz, 2H), 3.88 (s, 3H), 2.63 ppm (s, 3H); ^{13}C NMR ($CDCl_3$, 75 MHz): δ = 188.5, 182.7, 163.6, 156.4, 152.9, 143.7, 139.7, 135.4, 131.8, 131.2, 131.0, 130.9, 129.0, 128.6, 127.1, 123.6, 121.8, 121.7, 116.6, 114.0, 55.6, 15.3 ppm; ESIMS (*m/z*): 431 $[M+H]^+$; HRMS *m/z* calcd for $C_{26}H_{19}ClO_4$ $[M+H]^+$ 431.1050, found 431.1036.

(*E*)-3-(2-(4-Chlorobenzoyl)-7-methylbenzofuran-5-yl)-1-(4-chlorophenyl)prop-2-en-1-one (4b): This compound was synthesized by the method described for compound **4a**, employing 2-(4-chlorobenzoyl)-7-methylbenzofuran-5-carbaldehyde (**3a**) (1.0 g, 3.35 mmol), 4-chloroacetophenone (0.6 g, 4.02 mmol) and 10% methanolic KOH (15 mL) to afford compound **4b**. Pale-yellow solid; yield: 65%, 0.94 g; mp: 156–157 °C; $\tilde{\nu}_{max}$ (KBr) = 3015, 2935, 1700, 1662, 1570, 1530, 1274, 756 cm^{-1}; ^{1}H NMR ($CDCl_3$, 300 MHz): δ = 8.06–7.98 (m, 4H), 7.90 (d, J = 15.5 Hz, 1H), 7.81 (s, 1H), 7.63 (s, 1H), 7.56–7.47 (m, 6H), 2.65 (s, 3H); ^{13}C NMR ($CDCl_3$, 75 MHz): δ = 188.7, 182.4, 144.8, 139.5, 139.1, 136.3, 131.0, 130.7, 129.7, 128.8, 128.3, 126.9, 123.5, 121.9, 120.9, 116.2, 15.0 ppm; ESIMS (*m/z*): 435 $[M+H]^+$; HRMS *m/z* calcd for $C_{25}H_{16}Cl_2O_3$ $[M+H]^+$ 435.0555, found 435.0560.

(*E*)-3-(2-(4-Chlorobenzoyl)-7-methylbenzofuran-5-yl)-1-phenylprop-2-en-1-one (4c): This compound was synthesized by the method described for compound **4a**, employing 2-(4-chlorobenzoyl)-7-methylbenzofuran-5-carbaldehyde (**3a**) (1.0 g, 3.35 mmol), acetophenone (0.4 g, 4.02 mmol) and 10% methanolic KOH (15 mL) to afford compound **4c**. Yellow solid; yield: 70%, 0.93 g; mp: 179–180 °C; $\tilde{\nu}_{max}$ (KBr) = 3030, 2925, 1730, 1613, 1561, 1548, 1253, 770 cm^{-1}; ^{1}H NMR ($CDCl_3$, 300 MHz): δ = 8.05–8.02 (m, 4H), 7.88 (d, J = 15.6 Hz, 1H), 7.79 (s, 1H), 7.62 (s, 1H), 7.59–7.48 (m, 7H), 2.63 ppm (s, 3H); ^{13}C NMR ($CDCl_3$, 75 MHz): δ = 190.3, 182.6, 156.4, 152.9, 144.6, 139.7, 138.3, 135.3, 132.9, 131.5, 131.0, 129.0, 128.7, 128.7, 128.6, 127.1, 123.6, 122.0, 121.8, 116.6, 15.3 ppm; ESIMS (*m/z*): 401 $[M+H]^+$; HRMS *m/z* calcd for $C_{25}H_{17}ClO_3$ $[M+H]^+$ 401.0944, found 401.0920.

(*E*)-3-(2-(4-Chlorobenzoyl)-7-methylbenzofuran-5-yl)-1-*p*-tolylprop-2-en-1-one (4d): This compound was synthesized by the method described for compound **4a**, employing 2-(4-chlorobenzoyl)-7-methylbenzofuran-5-carbaldehyde (**3a**) (1.0 g, 3.35 mmol), 4-methylacetophenone (0.5 g, 3.95 mmol) and 10% methanolic KOH (15 mL) to afford compound **4d**. Pale-yellow solid; yield: 75%, 1.03 g; mp: 160–161 °C; $\tilde{\nu}_{max}$ (KBr) = 3043, 2912, 1670, 1580, 1532, 1215, 1246, 751 cm^{-1}; ^{1}H NMR ($CDCl_3$, 300 MHz): δ = 8.04 (d, J = 8.64 Hz, 2H), 7.96 (d, J = 8.0 Hz, 2H), 7.88 (d, 1H, J = 15.6 Hz), 7.80 (s, 1H), 7.63 (s, 1H), 7.57–7.51 (m, 4H), 7.31 (d, J = 8.0 Hz, 2H), 2.64 (s, 3H), 2.44 ppm (s, 3H); ^{13}C NMR ($CDCl_3$, 75 MHz): δ = 189.7, 182.6, 156.4, 152.9, 144.1, 143.8, 139.7, 135.7, 135.3, 131.6, 131.0, 129.4, 129.0, 128.7, 128.6, 127.1, 123.6, 127.1, 123.6, 121.9, 121.8, 116.6, 21.7, 15.3 ppm; ESIMS (*m/z*): 415 $[M+H]^+$; HRMS *m/z* calcd for $C_{26}H_{19}ClO_3$ $[M+H]^+$ 415.1101, found 415.1116.

(*E*)-3-(7-Methyl-2-(4-methylbenzoyl)benzofuran-5-yl)-1-*p*-tolylprop-2-en-1-one (4e): This compound was synthesized by the method described for compound **4a**, employing 7-methyl-2-(4-methylbenzoyl)benzofuran-5-carbaldehyde (**3b**) (1.0 g, 3.59 mmol), 4-methylacetophenone (0.5 g, 4.25 mmol) and 10% methanolic KOH (15 mL) to afford compound **4e**. Pale-yellow solid; yield: 68%, 0.95 g; mp: 137–138 °C; $\tilde{\nu}_{max}$ (KBr) = 3038, 2942, 1689, 1598, 1549, 716 cm^{-1}; ^{1}H NMR ($CDCl_3$, 300 MHz): δ = 8.01–7.96 (m, 4H), 7.89 (d, J = 15.6 Hz, 1H), 7.80 (s, 1H), 7.63 (s, 1H), 7.58–7.53 (m, 2H), 7.37–7.31 (m, 4H), 2.66 (s, 3H), 2.48–2.45 ppm (m, 6H); ^{13}C NMR ($CDCl_3$,

75 MHz): δ = 189.8, 183.8, 156.3, 153.3, 144.3, 144.1, 143.7, 135.8, 134.5, 131.4, 129.8, 129.5, 129.4, 128.7, 128.3, 127.3, 123.6, 121.9, 121.7, 116.2, 21.9, 21.8, 15.3 ppm; ESIMS (*m/z*): 395 $[M+H]^+$; HRMS *m/z* calcd for $C_{27}H_{22}O_3$ $[M+H]^+$ 395.1647, found 395.1638.

(*E*)-3-(7-Methyl-2-(4-methylbenzoyl)benzofuran-5-yl)-1-phenylprop-2-en-1-one (4f): This compound was synthesized by the method described for compound **4a**, employing 7-methyl-2-(4-methylbenzoyl)benzofuran-5-carbaldehyde (**3b**) (1.0 g, 3.59 mmol), acetophenone (0.5 g, 4.20 mmol) and 10% methanolic KOH (15 mL) to afford compound **4f**. Yellow solid; yield: 73%, 0.99 g; mp: 170–171 °C; $\tilde{\nu}_{max}$ (KBr) = 3012, 2938, 1645, 1588, 1527, 785 cm^{-1}; ^1H NMR ($CDCl_3$, 300 MHz): δ = 8.06–7.98 (m, 4H), 7.89 (d, *J* = 15.6 Hz, 1H), 7.80 (s, 1H), 7.62–7.49 (m, 6H), 7.35 (d, *J* = 7.9 Hz, 2H), 2.65 (s, 3H), 2.47 ppm (s, 3H); ^{13}C NMR ($CDCl_3$, 75 MHz): δ = 190.3, 183.7, 156.4, 153.4, 144.8, 144.1, 138.3, 134.5, 132.9, 131.3, 129.8, 129.4, 128.7, 128.6, 128.3, 127.3, 123.6, 121.9, 121.6, 116.2, 21.8, 15.3 ppm; ESIMS (*m/z*): 381 $[M+H]^+$; HRMS *m/z* calcd for $C_{26}H_{20}O_3$ $[M+H]^+$ 381.1491, found 381.1479.

(*E*)-1-(4-Methoxyphenyl)-3-(7-methyl-2-(4-methylbenzoyl)benzofuran-5-yl)prop-2-en-1-one (4g): This compound was synthesized by the method described for compound **4a**, employing 7-methyl-2-(4-methylbenzoyl)benzofuran-5-carbaldehyde (**3b**) (1.0 g, 3.59 mmol), 4-methoxylacetophenone (0.6 g, 4.31 mmol) and 10% methanolic KOH (15 mL) to afford compound **4g**. Pale-yellow solid, yield: 65%, 0.95 g; mp: 190–191 °C; $\tilde{\nu}_{max}$ (KBr) = 3036, 2948, 1600, 1209, 720 cm^{-1}; ^1H NMR ($CDCl_3$, 300 MHz): δ = 8.03 (d, *J* = 8.7 Hz, 2H), 7.94 (d, 2H, *J* = 8.0 Hz), 7.88 (d, 1H, *J* = 15.0 Hz), 7.79 (s, 1H), 7.62 (s, 1H), 7.58–7.52 (m, 2H), 7.35 (d, *J* = 7.92 Hz, 2H), 6.99 (d, *J* = 8.7 Hz, 2H), 3.90 (s, 3H), 2.65 (s, 3H), 2.47 ppm (s, 3H); ^{13}C NMR ($CDCl_3$, 75 MHz): δ = 188.5, 183.8, 163.5, 156.3, 153.2, 144.1, 143.9, 134.5, 131.4, 131.1, 130.9, 129.7, 129.4, 128.3, 127.2, 123.5, 121.9, 121.3, 116.3, 113.9, 55.6, 21.8, 15.4 ppm; ESIMS (*m/z*): 411 $[M+H]^+$; HRMS *m/z* calcd for $C_{27}H_{22}O_4$ $[M+H]^+$ 411.1596, found 411.1576.

(*E*)-3-(2-Benzoyl-7-methylbenzofuran-5-yl)-1-*p*-tolylprop-2-en-1-one (4h): This compound was synthesized by the method described for compound **4a**, employing 2-benzoyl-7-methylbenzofuran-5-carbaldehyde (**3c**) (1.0 g, 3.78 mmol), 4-methylacetophenone (0.6 g, 4.54 mmol) and 10% methanolic KOH (15 mL) to afford compound **4h**. Yellow solid; yield: 68%, 0.97 g; mp: 168–169 °C; $\tilde{\nu}_{max}$ (KBr) = 3008, 2915, 1648, 1570, 1559, 736 cm^{-1}; ^1H NMR ($CDCl_3$, 300 MHz): δ = 8.07–8.04 (m, 2H), 7.96 (d, *J* = 8.0 Hz, 2H), 7.88 (d, *J* = 15.6 Hz, 1H), 7.79 (s, 1H), 7.67–7.62 (m, 2H), 7.57–7.51 (m, 4H), 7.31 (d, *J* = 8.0 Hz, 2H), 2.65 (s, 3H), 2.44 ppm (s, 3H); ^{13}C NMR ($CDCl_3$, 75 MHz): δ = 189.7, 184.1, 156.4, 153.1, 144.2, 143.7, 137.2, 135.7, 133.1, 131.5, 129.5, 129.4, 128.8, 128.7, 128.5, 127.2, 123.6, 121.9, 121.7, 116.7, 21.7, 15.3 ppm; ESIMS (*m/z*): 381 $[M+H]^+$; HRMS *m/z* calcd for $C_{26}H_{20}O_3$ $[M+H]^+$ 381.1491, found 381.1503.

(*E*)-3-(2-Benzoyl-7-methylbenzofuran-5-yl)-1-phenylprop-2-en-1-one (4i): This compound was synthesized by the method described for compound **4a**, employing 2-benzoyl-7-methylbenzofuran-5-carbaldehyde (**3c**) (1.0 g, 3.78 mmol), acetophenone (0.6 g, 4.54 mmol) and 10% methanolic KOH (15 mL) to afford compound **4i**. Pale-yellow solid; yield: 75%, 1.03 g; mp: 180–181 °C; $\tilde{\nu}_{max}$ (KBr) = 3047, 2928, 1680, 1555, 1512, 758 cm^{-1}; ^1H NMR ($CDCl_3$, 300 MHz) δ = 8.08–8.03 (m, 4H), 7.90 (d, *J* = 15.6 Hz, 1H), 7.80 (s, 1H), 7.65–7.52 (m, 9H), 2.66 ppm (s, 3H); ^{13}C NMR ($CDCl_3$, 75 MHz): δ = 190.4, 184.2, 156.5, 153.0, 144.7, 138.2, 137.1, 133.1, 132.9, 131.3, 129.5, 128.8, 128.7, 128.6, 128.5, 127.2, 123.7, 122.1, 121.6, 116.8, 15.4 ppm; ESIMS (*m/z*): 367 $[M+H]^+$; HRMS *m/z* calcd for $C_{25}H_{18}O_3$ $[M+H]^+$ 367.1334, found 367.1339.

(*E*)-3-(2-(4-Chlorobenzoyl)-7-methylbenzofuran-5-yl)-1-(3,4,5-trimethoxyphenyl)prop-2-en-1-one (4j): This compound was synthesized by the method described for compound **4a**, employing 2-(4-chlorobenzoyl)-7-methylbenzofuran-5-carbaldehyde (**3a**) (1.0 g, 3.35 mmol), 3,4,5-trimethoxyacetophenone (0.8 g, 4.02 mmol) and 10% methanolic KOH (15 mL) to afford compound **4j**. Yellow solid; yield: 66%, 1.08 g; mp: 140–141 °C; $\tilde{\nu}_{max}$ (KBr) = 3028, 2936, 1663, 1566, 1218, 701 cm^{-1}; ^1H NMR ($CDCl_3$, 300 MHz): δ = 8.06–8.03 (m, 2H), 7.90 (d, *J* = 15.42 Hz, 1H), 7.82 (s, 1H), 7.63 (s, 1H), 7.57–7.46 (m, 4H), 7.30–7.24 (m, 2H), 3.97–3.95 (m, 9H), 2.66 ppm (s, 3H); ^{13}C NMR ($CDCl_3$, 75 MHz): δ = 188.5, 184.2, 163.5, 156.3, 152.9, 143.8, 138.4, 137.1, 133.1, 133.0, 131.5, 131.4, 131.1, 130.9, 129.5, 128.7, 128.4, 127.1, 123.6, 122.0, 121.3, 116.9, 113.9, 55.6, 15.4 ppm; ESIMS (*m/z*): 491 $[M+H]^+$; HRMS *m/z* calcd for $C_{28}H_{23}ClO_6$ $[M+H]^+$ 491.1261, found 491.1264.

(*E*)-3-(2-Benzoyl-7-methylbenzofuran-5-yl)-1-(4-chlorophenyl)prop-2-en-1-one (4k): This compound was synthesized by the method described for compound **4a**, employing 2-benzoyl-7-methylbenzofuran-5-carbaldehyde (**3c**) (1.0 g, 3.78 mmol), 4-chloroacetophenone (0.6 g, 4.54 mmol) and 10% methanolic KOH (15 mL) to afford compound **4k**. Pale-yellow solid; yield: 67%, 1.08 g; mp: 175–176 °C; $\tilde{\nu}_{max}$ (KBr) = 3032, 2943, 1736, 1676, 1566, 1218, 748 cm^{-1}; ^1H NMR ($CDCl_3$, 300 MHz): δ = 8.07–8.04 (m, 2H), 7.98 (d, *J* = 8.5 Hz, 2H), 7.89 (d, *J* = 15.6 Hz, 1H), 7.79 (s, 1H), 7.67–7.61 (m, 2H), 7.57–7.46 (m, 6H), 2.65 ppm (s, 3H); ^{13}C NMR ($CDCl_3$, 75 MHz): δ = 189.0, 184.1, 156.5, 153.2, 145.2, 139.3, 137.2, 136.6, 133.2, 131.2, 130.0, 129.6, 128.7, 128.5, 127.3, 123.8, 122.2, 121.1, 116.6, 15.3 ppm; ESIMS (*m/z*): 401 $[M+H]^+$; HRMS *m/z* calcd for $C_{25}H_{17}ClO_3$ $[M+H]^+$ 401.0944, found 401.0936.

(*E*)-3-(7-Methyl-2-(4-methylbenzoyl)benzofuran-5-yl)-1-(thiophen-2-yl)prop-2-en-1-one (4l): This compound was synthesized by the method described for compound **4a**, employing 7-methyl-2-(4-methylbenzoyl)benzofuran-5-carbaldehyde (**3b**) (1.0 g, 3.59 mmol), 4-acetylthiophene (0.5 g, 4.31 mmol) and 10% methanolic KOH (15 mL) to afford compound **4l**. Pale-yellow solid; yield: 76%, 1.04 g; mp: 130–131 °C; $\tilde{\nu}_{max}$ (KBr) = 3012, 2921, 2925, 1710, 1627, 1210, 719 cm^{-1}; ^1H NMR ($CDCl_3$, 300 MHz): δ = 8.00–7.89 (m, 4H), 7.80 (s, 1H), 7.69 (dd, *J* = 1.1, 4.9 Hz, 1H), 7.62 (s, 1H), 7.53 (s, 1H), 7.46–7.40 (m, 1H), 7.37–7.34 (m, 2H), 7.21–7.18 (m, 1H), 2.66 (s, 3H), 2.47 ppm (s, 3H); ^{13}C NMR ($CDCl_3$, 75 MHz): δ = 183.7, 181.9, 156.4, 153.3, 145.7, 144.0, 134.5, 134.0, 131.9, 131.1, 129.8, 129.4, 128.3, 127.3, 123.6, 122.0, 121.2, 116.2, 21.8, 15.3; ESIMS (*m/z*): 387 $[M+H]^+$; HRMS *m/z* calcd for $C_{24}H_{18}O_3S$ $[M+H]^+$ 387.1055, found 387.1051.

(*E*)-3-(2-Benzoyl-7-methylbenzofuran-5-yl)-1-(thiophen-2-yl)prop-2-en-1-one (4m): This compound was synthesized by the method described for compound **4a**, employing 2-benzoyl-7-methylbenzofuran-5-carbaldehyde (**3c**) (1.0 g, 3.78 mmol), 2-acetylthiophene (0.5 g, 4.54 mmol) and 10% methanolic KOH (15 mL) to afford compound **4m**. Pale-yellow solid; yield: 78%, 1.09 g; mp: 110–111 °C; $\tilde{\nu}_{max}$ (KBr) = 3027, 2944, 2858, 1736, 1623, 1248, 742 cm^{-1}; ^1H NMR ($CDCl_3$, 300 MHz): δ = 8.08–8.04 (m, 2H), 7.96–7.89 (m, 2H), 7.80 (s, 1H), 7.69 (dd, *J* = 1.1, 4.9 Hz, 1H), 7.65–7.63 (m, 2H), 7.58–7.53 (m, 3H), 7.43 (d, *J* = 15.5 Hz, 1H), 7.21–7.18 (m, 1H), 2.66 ppm (s, 3H); ^{13}C NMR ($CDCl_3$, 75 MHz): δ = 184.1, 181.9, 156.4, 153.0, 145.6, 143.9, 137.1, 134.0, 133.1, 131.9, 131.1, 129.5, 128.7, 128.5, 128.3, 127.2, 123.7, 122.2, 121.1, 116.8, 15.3 ppm; ESIMS (*m/z*): 373 $[M+H]^+$; HRMS *m/z* calcd for $C_{23}H_{16}O_3S$ $[M+H]^+$ 373.0898, found 373.0896.

Biological methods

C. elegans strains and maintenance: Genetic model system *C. elegans* was employed to study the biological effects of the test compounds. Wild-type strain N2 (var. Bristol) and transgenic strains CL4176 and CL2006 expressing human Aβ, LX929 expressing GFP in all cholinergic neurons, were employed for the studies. The strains were obtained from the *Caenorhabditis* Genetics Center (University of Minnesota, USA). The culture and maintenance of various *C. elegans* strains was carried out as per standard methods.[47] Briefly, the strains were cultured on bacterial lawns of OP50-seeded nutrient growth medium (NGM) plates at 22 °C. Strain CL4176 was maintained at 16 °C. NGM was prepared by adding 50 mM NaCl, 2.5 g L^{-1} peptone (Sigma), 17 g L^{-1} agar (Hi-media) in 975 mL double-distilled water and autoclaved for 30–40 min at 15 psi. After the cooling of media to 50–60 °C, 5 μg mL^{-1} cholesterol solution (Sigma) prepared in ethanol, 1 mM $CaCl_2$, 1 mM $MgSO_4$, and 25 mM KH_2PO_4 were added. On the day of initiation of treatment, worms were synchronized by hypochlorite bleaching method[48] for the isolation of embryos.

Treatment of worms with test compounds: Test compounds were initially dissolved in ethanol to prepare a stock of 20 mM. A working concentration of 2 mM was then prepared from the stock in OP50, followed by seeding it onto NGM plates and incubated overnight at 37 °C. Embryos of worms were transferred onto OP50–test-compound-seeded plates and grown for 48 h.

Analysis of Aβ aggregation: Aβ-induced paralysis assays were carried out as per a published method[49] with slight modifications. In this study, we used temperature-inducible Aβ-expressing transgenic CL4176 strains of *C. elegans*. The strain expresses Aβ specifically in muscles, and increased Aβ expression leads to paralysis. This gives an easy endpoint to carry out large scale analysis of compounds for their effect against Aβ aggregation. Age-synchronized CL4176 worms were grown on NGM plates seeded with OP50 and premixed with test compounds for 48 h at 16 °C. After 48 h the temperature was increased to 25 °C for another 36 h to induce expression of Aβ, leading to paralysis. The scoring of paralysis was carried out by comparing each test-compound-treated group with control. Paralysis phenotype was counted for ~50 worms per treatment condition. The assays were repeated thrice, and the data for each compound were statistically analyzed and plotted against control values.

Aldicarb assay for effect on excitatory neurotransmission: The compounds exhibiting a positive effect in the Aβ aggregation assay were further studied for their effect on availability of excitatory neurotransmitter ACh, which holds immense significance in the treatment of AD. The aldicarb assay was carried out as described previously.[50] In brief, 1 M stock solution of aldicarb (Fluka Cat.# 33386) was prepared in 70% ethanol. NGM–aldicarb plates were prepared at least one day before to get a final concentration of 1 mM aldicarb in NGM and stored at 4 °C until use. Embryos of wild-type (N2) worms were transferred onto OP50-seeded control plates and test-compound-seeded NGM plates at 22 °C. After 48 h treatment, the control or treated worms were washed off their parent plates to remove the adhering bacteria and transferred onto the aldicarb assay plates (20–30 worms per plate). The worms were poked with a poking lash (prepared by fixing an eye lash at the tip of a microtip). The paralysis phenotype of worms was scored at a fixed time point, and the percentage of worms paralyzed under treated conditions was normalized against control values. Assays were repeated thrice.

Estimation of ACh and AChE activities with Amplex® Red: We quantified the levels of ACh and AChE in wild-type worms treated with compounds **4f**, **4i**, and **4m**. After treatment for 48 h, worms were washed thrice with sodium phosphate buffer (PBS) to remove adhering bacteria. Worms were homogenized by sonication on ice at 15 s intervals using 25% amplitude. Samples were then centrifuged at 14000 rpm for 30 min to remove any insoluble residue. The supernatant was assayed for ACh and AChE levels using the Amplex® Red ACh/AChE assay kit (Invitrogen Cat.# A12217) according to the manufacturer's instructions. Absorbance was measured in a microplate reader with an excitation wavelength of 544 nm and an emission wavelength of 590 nm.[51] Experiments were performed in triplicates at two different times, and final fluorescence was normalized with respect to protein content as quantified using the Bradford method.

Estimation of oxidative stress: We carried out 2,7-dichlorodihydrofluorescein diacetate (H_2DCFDA) (Invitrogen Cat.# D399) assays to determine the levels of ROS using standard protocols.[52] After treatment for 48 h, control and treated worms of CL2006 strains were washed thrice with M9 buffer to remove bacteria. Approximately 100 worms per 100 μL of buffer were pipetted in four replicates into the wells of a 96-well plate; then 100 μL of 100 μM H_2DCFDA was added to each well, and basal fluorescence was quantified immediately after addition of dye with an excitation wavelength of 485 nm and an emission wavelength of 520 nm. Plates were incubated for 1 h and then a second measurement was quantified. The initial fluorescence was subtracted from the second reading, and the fluorescence per 100 worms was calculated by dividing the delta by number of worms. The experiment was repeated twice and the average was considered.

Analysis of cholinergic neurodegeneration: Cholinergic neurodegeneration was induced by treatment of worms with an organophosphate insecticide chlorpyrifos (CP; Riedel–de Haën Cat.# 45395). It was mixed with OP50 at 100 ppm concentration and seeded onto NGM plates and incubated overnight at 37 °C. Initially, we employed four different concentrations of CP: 1, 10, 100, and 1000 ppm in order to determine the concentration that induces cholinergic neurodegeneration without causing mortality in worms. Age-synchronized worms of LX929 were then grown on normal diet or treatment plates for 48 h at 22 °C. After this, worms were washed thrice using M9 buffer followed by mounting the worms onto a 2% agar-padded glass slide using 100 mM NaN_3 (Sigma Cat.# 71289). Imaging of live (anesthetized) worms was carried out to monitor the cholinergic neurodegeneration in control and experimental conditions using a fluorescence upright microscope (Nikon). Ten subjects were analyzed per group, and the experiment was repeated twice. Fluorescence intensity was quantified using Image J software (Image J, US National Institutes of Health (NIH), Bethesda, MD, USA).

Quantification of lipid content: Nile red staining of lipid deposits was performed as described previously.[47] This lipid-specific Nile red dye (Invitrogen Cat.# N1142) was mixed with *E. coli* OP50 at a ratio of 1:250. The synchronously aged embryos of CL2006 derived from axenizing by hypochlorite treatment, were fed onto these Nile-red-containing treatment plates for 48 h at 22 °C. Worms were washed off and mounted using NaN_3 on a glass slide with a cover slip. Imaging of ten live (immobilized) worms was carried out using a fluorescence upright microscope (Nikon). Images of Nile red staining were further quantified using Image J software (Image J, NIH) by measuring florescence intensity.

Mitotracker staining for mitochondrial content: Mitotracker deep red 633 stain solution (Invitrogen Cat.#: M-22426) was prepared in OP50 to reach a concentration of 100 nM. OP50–stain solution was seeded onto NGM plates and incubated overnight at 37 °C. Embryos of N2 and CL2006 worms were transferred onto the NGM–OP50 stain solution and grown for 48 h at 22 °C. Worms were washed from plates, cleared off any adhering bacteria and immobilized in 100 mM NaN_3 on a glass slide and analyzed at room temperature at a laser excitation wavelength of 637 nm and an emission wavelength of 660 nm (confocal microscope, Carl Zeiss).[53] We analyzed 10 worms per group, and experiments were repeated twice. Images were further quantified by measuring florescence intensity using Image J Software (Image J, NIH).

Trypan-blue-based dye exclusion test for studies on tissue/cell damage in C. elegans: In this assay, worms treated with different compounds and Paraquat (PQ; positive control) were studied. In PQ treatment, age-synchronized worms were grown onto the PQ–OP50-seeded NGM plates at 4 mM, and the staining was performed as described previously with slight modifications.[54] After treatment for 48 h, worms were washed thrice using M9 buffer to remove any adhering bacteria and transferred onto a watch glass, wherein 300 μL Trypan blue stain (14 mg mL^{-1}; Sigma Cat.# T6146-5g) was added. The samples were incubated for 20 min with continuous shaking on an orbital shaker. Worms were washed thrice with M9 buffer at 3000 rpm for 2 min and then kept in the shaker for 5 min for de-staining in M9. Worms were finally mounted on agar-padded slides and observed (10 worms per treatment condition) for staining pattern under a microscope (Nikon). Each experiment was carried out in triplicate.

Thioflavin S staining of Aβ: For thioflavin S staining, individual transgenic animals from treatment plates were washed thrice using M9 buffer and were fixed in 4% paraformaldehyde in PBS overnight at 4 °C. Afterward, worms were freeze-fractured by placing worms between two microscope slides, and quick-frozen at −45 °C. The slides were cracked off from one another. Worms were then permeabilized by incubation in 200 μL permeabilization solution (5% fresh β-mercaptoethanol, 1% Triton X-100, 125 mM Tris, pH 7.4) for 48 h at 37 °C. Permeabilized worms were finally washed with PBST (0.1% Triton in PBS) and subjected to staining by transfer to 0.125% thioflavin S (Sigma) in 50% ethanol for 2 min, de-stained for 2 min in 50% ethanol, followed by washing twice in 50% ethanol and mounted on a microscope slide with 50% glycerol. Aβ fluorescence images were acquired using a 40× objective (Carl Zeiss) equipped with a digital camera.[55] Further quantitative analyses of Aβ deposits in the transgenic *C. elegans* strain CL2006, expressed as mean number of Aβ deposits per worm, were carried out.

Data analysis: All results are given as the mean ± standard error of the mean (SEM). Differences between groups were analyzed statistically employing Student's t test using the GraphPad Prism 5 software package.

Docking evaluation

For docking studies, we considered the X-ray crystal structure of *Torpedo californica* AChE (PDB ID: 1EVE) in complex with E2020. AutoDock 4.055 integrated with MGL tools 1.5 was used for docking simulation. See the Supporting Information for further details.

Crystal structure data for compound 4d

CCDC-877579 contains the supplementary crystallographic data for this paper. These data can be obtained free of charge from The Cambridge Crystallographic Data Centre via www.ccdc.cam.ac.uk/data_request/cif.

Abbreviations

Aβ: β-amyloid peptide; ACh: acetylcholine; AChE: acetylcholinesterase; AD: Alzheimer's disease; CNS: central nervous system; CP: chlorpyrifos; ESIMS: electrospray ionization mass spectrometry; HMTA: hexamethylenetetraamine; HPLC: high-performance liquid chromatography; HRMS: high-resolution mass spectrometry; H_2DCFDA: 2,7-dichlorodihydrofluorescein diacetate; MTDL: multi-target-directed ligand; NGM: nutrient growth medium; PS-1: presenilin-1; ROS: reactive oxygen species; SAR: structure–activity relationship; TFA: trifluoroacetic acid; TLC: thin-layer chromatography; TMS: tetramethylsilane.

Acknowledgements

The instrumentation facilities at the Sophisticated Analytical Instrument Facility (SAIF) of the Central Drug Research Institute (CDRI) are gratefully acknowledged. M.K., R.K.M., and P.J. are thankful to the Council of Scientific and Industrial Research (CSIR), New Delhi (India) for financial support. Ram Jeet (CSIR-CDRI) is acknowledged for HPLC data, and Suriya P. Singh (CSIR-CDRI) is acknowledged for technical support. We are grateful to Dr. S. K. Puri (Director, CSIR-CDRI) for funding and for his constant encouragement in the drug discovery program. Nematode strains used in this work were provided by the C. elegans Genetics Center (CGC), University of Minnesota, MN (USA), which is funded by the US National Institutes of Health National Center for Research Resources (NIH–NCRR). This work is part 31 in the series, "Advances in drug design and discovery"; this is CSIR-CDRI communication number 8772.

Keywords: Alzheimer's disease · benzofurans · beta-amyloid · *Caenorhabditis elegans* · chalcones

[1] W. Thies, L. Bleiler, Alzheimer's Association, *Alzheimers Dement.* **2013**, *9*, 208 – 245.
[2] L. M. Ittner, J. Götz, *Nat. Rev. Neurosci.* **2011**, *12*, 65 – 72.
[3] M. T. Lin, M. F. Beal, *Nature* **2006**, *443*, 787 – 795.
[4] C. W. Lindsley, *ACS Chem. Neurosci.* **2012**, *3*, 804 – 805.
[5] M. Citron, *Nat. Rev. Drug Discovery* **2010**, *9*, 387 – 398.
[6] E. Callaway, *Nature* **2012**, *489*, 13 – 14.
[7] M. Bajda, N. Guzior, M. Ignasik, B. Malawska, *Curr. Med. Chem.* **2011**, *18*, 4949 – 4975.
[8] R. León, A. G. Garcia, J. Marco-Contelles, *Med. Res. Rev.* **2013**, *33*, 139 – 189.
[9] K. Mehnaz, K. S. Ashok, J. Talha, *Int. J. Med. Pharm. Sci.* **2011**, *1*, 1 – 15.
[10] J. Liu, V. Dumontet, A. L. Simonin, B. I. Iorga, V. Guerineau, M. Litaudon, V. H. Nguyen, F. Gueritte, *J. Nat. Prod.* **2011**, *74*, 2081 – 2088.
[11] a) D. R. Howlett, A. E. Perry, F. Godfrey, J. E. Swatton, K. H. Jennings, C. Spitzfaden, H. Wadsworth, S. J. Wood, R. E. Markwell, *Biochem. J.* **1999**, *340*, 283 – 289; b) S. Rizzo, C. Riviere, L. Piazzi, A. Bisi, S. Gobbi, M. Bartolini, V. Andrisano, F. Morroni, A. Tarozzi, J. P. Monti, A. Rampa, *J. Med. Chem.* **2008**, *51*, 2883 – 2886.
[12] J. H. Byun, H. Kim, Y. Kim, I. Mook-Jung, D. J. Kim, W. K. Lee, K. H. Yoo, *Bioorg. Med. Chem. Lett.* **2008**, *18*, 5591 – 5593.

[13] N. K. Sahu, S. S. Balbhadra, J. Choudhary, D. V. Kohli, *Curr. Med. Chem.* **2012**, *19*, 209 – 225.
[14] S. Vogel, S. Ohmayer, G. Brunner, J. Heilmann, *Bioorg. Med. Chem.* **2008**, *16*, 4286 – 4293.
[15] a) S. Bayati, R. Yazdanparast, S. S. Majd, S. Oh, *J. Appl. Toxicol.* **2011**, *31*, 545 – 553; b) C. Chiruta, D. Schubert, R. Dargusch, P. Maher, *J. Med. Chem.* **2012**, *55*, 378 – 389.
[16] F. Yang, G. P. Lim, A. N. Begum, O. J. Ubeda, M. R. Simmons, S. S. Ambegaokar, P. P. Chen, R. Kaved, C. G. Glabe, S. A. Frautschy, G. M. Cole, *J. Biol. Chem.* **2005**, *280*, 5892 – 5901.
[17] A. Rampa, F. Belluti, S. Gobbi, A. Bisi, *Curr. Top. Med. Chem.* **2011**, *11*, 2716 – 2730.
[18] K. V. Sashidhara, M. Kumar, V. Khedgikar, P. Kushwaha, R. K. Modukuri, A. Kumar, J. Gautam, D. Singh, B. Sridhar, R. Trivedi, *J. Med. Chem.* **2013**, *56*, 109 – 122.
[19] a) K. V. Sashidhara, M. Kumar, R. Sonkar, B. S. Singh, A. K. Khanna, G. Bhatia, *J. Med. Chem.* **2012**, *55*, 2769 – 2779; b) K. V. Sashidhara, R. K. Modukuri, Pooja Jadiya, K. B. Rao, T. Sharma, R. Haque, D. K. Singh, D. Banerjee, M. I. Siddiqi, A. Nazir, *ACS Med. Chem. Lett.* **2014**, DOI: 10.1021/ml500222g.
[20] C. D. Link, *Proc. Natl. Acad. Sci. USA* **1995**, *92*, 9368 – 9372.
[21] a) T. Kaletta, M. O. Hengartner, *Nat. Rev. Drug Discovery* **2006**, *5*, 387 – 398; b) A. K. Jones, S. D. Buckingham, D. B. Sattelle, *Nat. Rev. Drug Discovery* **2005**, *4*, 321 – 330.
[22] W. Yanjue, L. Yuan, *Curr. Alzheimer Res.* **2005**, *2*, 37 – 45.
[23] D. Levitan, I. Greenwald, *Nature* **1995**, *377*, 351 – 354.
[24] a) N. Naik, K. H. Vijay, S. M. Dias, S. J. Ranga, *Int. J. Pharm. Pharm. Sci.* **2013**, *5*, 242 – 247; b) D. V. Singh, A. R. Mishra, R. M. Mishra, A. K. Pandey, C. R. Singh, A. K. Dwivedi, *Indian J. Pharm. Sci.* **2004**, *66*, 647 – 652.
[25] K. V. Sashidhara, R. K. Modukuri, R. Sonkar, K. B. Rao, G. Bhatia, *Eur. J. Med. Chem.* **2013**, *68*, 38 – 46.
[26] J. R. Stille, J. A. Ward, C. Leffelman, K. A. Sullivan, *Tetrahedron Lett.* **1996**, *37*, 9267 – 9270.
[27] W. H. W. Lunn, J. A. Monn, D. M. Zimmerman, (Eli Lilly & Co.), US Pat. No. 5,552,426 A, **1996**.
[28] Y. Ikarashi, Y. Harigaya, Y. Tomidokoro, M. Kanai, M. Ikeda, E. Matsubara, T. Kawarabayashi, H. Kuribara, S. G. Younkin, Y. Maruyama, M. Shoji, *Neurobiol. Aging* **2004**, *25*, 483 – 490.
[29] D. Qiao, F. J. Seidler, T. A. Slotkin, *Toxicol. Appl. Pharmacol.* **2005**, *206*, 17 – 26.
[30] J. G. Salazar, D. Ribes, M. Cabre, J. L. Domingo, F. Sanchez-Santed, M. T. Colomina, *Curr. Alzheimer Res.* **2011**, *8*, 732 – 740.
[31] D. Qiao, F. J. Seidler, C. A. Tate, M. M. Cousins, T. A. Slotkin, *Environ. Health Perspect.* **2003**, *111*, 536 – 544.
[32] T. S. Roy, V. Sharma, F. J. Seidler, T. A. Slotkin, *Brain Res. Dev. Brain Res.* **2005**, *155*, 71 – 80.
[33] M. Lotti, A. Moretto, *Toxicol. Rev.* **2005**, *24*, 37 – 49.
[34] F. Gultekin, N. Delibas, S. Yasar, I. Kilinc, *Arch. Toxicol.* **2001**, *75*, 88 – 96.
[35] M. S. Parihar, T. Hemnani, *J. Clin. Neurosci.* **2004**, *11*, 456 – 467.
[36] S. Alavez, M. C. Vantipalli, D. J. Zucker, I. M. Klang, G. J. Lithgow, *Nature* **2011**, *472*, 226 – 229.
[37] K. Leuner, T. Schutt, C. Kurz, S. H. Eckert, C. Schiller, A. Occhipinti, S. Mai, M. Jendrach, G. P. Eckert, S. E. Kruse, R. D. Palmiter, U. Brandt, S. Drose, I. Wittig, M. Willem, C. Haass, A. S. Reichert, W. E. Muller, *Antioxid. Redox Signaling* **2012**, *16*, 1421 – 1433.
[38] a) S. Jinno, N. Otsuka, T. Okita, K. Inouye, *Chem. Pharm. Bull.* **1999**, *47*, 1276 – 1283; b) S. S. Rindhe, M. A. Rode, B. K. Karale, *Indian J. Pharm. Sci.* **2010**, *72*, 231 – 235.
[39] A. Bindoli, M. P. Rigobello, E. Musacchio, R. Scuri, V. Rizzoli, L. Galzigna, *Pharm. Res.* **1991**, *24*, 369 – 375.
[40] a) T. Matsuzaki, K. Sasaki, J. Hata, Y. Hirakawa, K. Fujimi, T. Ninomiya, S. O. Suzuki, S. Kanba, Y. Kiyohara, T. Iwaki, *Neurology* **2011**, *77*, 1068 – 1075; b) M. Simons, P. Keller, B. De Strooper, K. Beyreuther, C. G. Dotti, K. Simons, *Proc. Natl. Acad. Sci. USA* **1998**, *95*, 6460 – 6464.
[41] a) M. P. Burns, W. J. Noble, V. Olm, K. Gaynor, E. Casey, J. La Francois, L. Wang, K. Duff, *Brain. Res. Mol. Brain. Res.* **2003**, *110*, 119 – 125; b) H. Hayashi, N. Kimura, H. Yamaguchi, K. Hasegawa, T. Yokoseki, M. Shibata, N. Yamamoto, M. Michikawa, Y. Yoshikawa, K. Terao, K. Matsuzaki, C. A. Lemere, D. J. Selkoe, H. Naiki, K. Yanagisawa, *J. Neurosci.* **2004**, *24*, 4894 – 4902.
[42] V. Vingtdeux, P. Chandakkar, H. Zhao, C. d'Abramo, P. Davies, P. Marambaud, *FASEB J.* **2011**, *25*, 219 – 231.
[43] G. Kryger, I. Silman, J. L. Sussman, *J. Physiol.* **1998**, *92*, 191 – 194.
[44] W. Luo, Q. S. Yu, S. S. Kulkarni, D. A. Parrish, H. W. Holloway, D. Tweedie, A. Shafferman, D. K. Lahiri, A. Brossi, N. H. Greig, *J. Med. Chem.* **2006**, *49*, 2174 – 2185.
[45] A. Saxena, J. M. Fedorko, C. R. Vinayaka, R. Medhekar, Z. Radic, P. Taylor, O. Lockridge, B. P. Doctor, *Eur. J. Biochem.* **2003**, *270*, 4447 – 4458.
[46] N. C. Inestrosa, A. Alvarez, C. A. Perez, R. D. Moreno, M. Vicente, C. Linker, O. I. Casanueva, C. Soto, J. Garido, *Neuron* **1996**, *16*, 881 – 891.
[47] P. Jadiya, M. Chatterjee, S. R. Sammi, S. Kaur, G. Palit, A. Nazir, *Biochem. Biophys. Res. Commun.* **2011**, *413*, 306 – 310.
[48] T. Stiernagle, *WormBook* **2006**, 1 – 11.
[49] C. Link, A. Taft, V. Kapulkin, K. Duke, S. Kim, Q. Fei, D. Wood, B. Sahagan, *Neurobiol. Aging* **2003**, *24*, 397 – 413.
[50] A. Nazir, S. R. Sammi, P. Singh, R. K. Tripathi, *PLoS One* **2010**, *5*, e15312.
[51] J. Chun-Hui, S. Eun-Joo, P. Jae-Bong, J. Choon-Gon, L. Zhengyi, K. Min-Soo, K. Kyo-Hwan, Y. Hyoung-Jong, P. Sang-Jae, C. Won-Cheol, Y. Kiyofumi, N. Toshitaka, K. Hyoung-Chun, *J. Neurosci. Res.* **2009**, *87*, 3658 – 3670.
[52] S. Kaur, S. R. Sammi, P. Jadiya, A. Nazir, *CNS Neurol. Disord. Drug Targets* **2012**, *11*, 387 – 394.
[53] M. Artal-Sanz, N. Tavernarakis, *Nature* **2009**, *461*, 793 – 797.
[54] L. Xuelan, C. Kezhou, F. Huiyun, Y. Hang, K. Mingguang, W. Lijun, W. Yuejin, Y. Zengliang, *Radiat. Environ. Biophys.* **2007**, *46*, 255 – 261.
[55] H. Levine III, *Methods Enzymol.* **1999**, *309*, 274 – 284.

Received: July 16, 2014
Published online on ■■ ■■, 0000

See *elegant* conjugates! To arrest multifaceted Alzheimer's disease, a series of multifunctional benzofuran–chalcone hybrids were synthesized and bio-evaluated using transgenic *C. elegans*. These hybrid compounds potently reduced the aggregation of β-amyloid peptide, increased the acetylcholine levels, and provided protection against neurodegeneration.

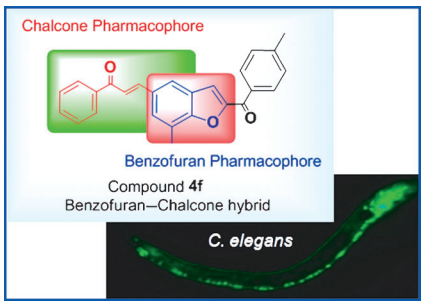

K. V. Sashidhara, R. K. Modukuri, P. Jadiya, R. P. Dodda, M. Kumar, B. Sridhar, V. Kumar, R. Haque, M. I. Siddiqi, A. Nazir**

■■ – ■■

Benzofuran–Chalcone Hybrids as Potential Multifunctional Agents against Alzheimer's Disease: Synthesis and in vivo Studies with Transgenic *Caenorhabditis elegans*